AXIALLY SYMMETRIC LAMINAR COMPRESSIBLE BOUNDARY LAYERS WITH PRESSURE GRADIENT

Joint Thesis by

Harry Frederick Imster

James Steven Lesko

In Partial Fulfillment of the Requirements

For the Degree of

Aeronautical Engineer

California Institute of Technology

Pasadena, California

1948

ACKNOWLEDGEMENT

The authors wish to express their appreciation to their advisor, Dr. H. J. Stewart, for his stimulating suggestions and constant interest in this study, to Dr. H. W. Liepmann for pointing out some helpful reference material, and to the typist, Margaret Brinkley, for her care and diligence in typing this manuscript.

SUMMARY

Previous work on the subject of laminar compressible boundary layers has considered the flat plate without a pressure gradient (Karman, Emmons and Brainerd), the flat plate with a pressure gradient (Illingworth), and the cone without pressure gradient (Hantzsche and Wendt). It is the purpose of this investigation to determine the effect of pressure gradient on the boundary layer thickness and skin friction for a figure of revolution in compressible flow.

The basic momentum, continuity, and energy equations of viscous, compressible flow are reduced to an approximate form in the neighborhood of the surface of a figure of revolution by the usual boundary layer assumptions and the particular assumptions that no heat is transferred between the figure of revolution and the fluid and that the Prandtl number is equal to unity. An integral relation is then developed for the approximate equations and is subsequently reduced to a differential equation in which the boundary layer thickness is the dependent variable. In addition to considering the case of compressible flow with a pressure gradient, three other cases are examined in order to aid in the interpretation of the results. These are: compressible flow with no pressure gradient, and incompressible flow with and without pressure gradient. The equations are then applied to a figure of revolution over which pressure distributions have been experimentally determined at two Mach numbers and two Reynolds numbers. The resulting boundary layer thickness distributions are then used to determine the skin friction drag for the various cases.

The effects of boundary layer velocity profile relation on skin

friction drag coefficient are considered in some detail.

The results of the investigation indicate that the usual practice of applying flat plate laminar skin friction drag coefficients (either compressible or incompressible) to figures of revolution in supersonic flow may be unconservative by a considerable margin. It is also shown that resulting drag values are considerably dependent on the boundary conditions used to obtain the boundary layer velocity profile.

TABLE OF CONTENTS

FIGURES

TABLES

INTRODUCTION

An extensive amount of literature exists on boundary layer investigations for incompressible flow. However, a comparatively small amount of effort has been directed towards determining viscous effects when compressibility can no longer be neglected.

Several theoretical investigations have been made of the laminar boundary layer on a flat plate in compressible flow with no pressure gradient. Among these studies are those of Emmons and Brainerd (reference 1), Busemann (reference 2), and Karman (reference 3). Busemann and Karman assume no heat transfer and Prandtl number of unity. Emmons and Brainerd also assume no heat transfer but include the effects of varying Prandtl number. Illingworth (reference 3a) has studied the laminar boundary layer on a flat plate in a supersonic flow with pressure gradient.

Mangler (reference 4) has shown that the behavior of the laminar boundary layer on a body of revolution in compressible flow can be calculated by solving a corresponding problem for two dimensional flow. The contour in the plane flow is determined by a suitable transformation. For the special case of supersonic flow towards a cone, Mangler's results agree with those of Hantzsche and Wendt (reference 5), in that the cone boundary layer thickness is smaller by a factor of $\sqrt{3}$ than the corresponding flat plate boundary layer thickness.

The aim of this study is to investigate the boundary layer behavior and skin friction for a body of revolution at zero angle of incidence in a compressible flow with pressure gradient. The

method of attack is similar to that employed by Millikan (reference 6) for incompressible flow, i.e., the basic integral relations are developed and are solved by the Polhausen method, assuming no heat transfer and Prandtl number of unity. Specific examples are calculated to determine the effects of,

(a) pressure gradient,

(b) compressibility, and

(c) assumed velocity profile

on the boundary layer thickness and skin friction drag of the V-2 ogive. These results are compared with values obtained from the Blasius solution for incompressible flow and the Emmons and Brainerd calculations for compressible flow over a flat plate with no pressure gradient.

NOMENCLATURE

r = radial distance from axis of symmetry.

r_o = radial distance from axis of symmetry to body surface.

n = normal distance from surface of body.

s = distance along surface of body from nose.

θ = azimuth angle.

β = angle between tangent to body surface and axis of symmetry.

A = wetted surface area.

L = body length.

δ = nominal boundary layer thickness.

η = $\frac{n}{\delta}$

p = local static pressure.

p_∞ = free stream static pressure.

p_o = stagnation pressure.

ρ = local density

ρ_∞ = free stream density.

ρ_o = free stream stagnation density.

T = local temperature (absolute).

T_∞ = free stream temperature (absolute).

T_o = stagnation temperature (absolute).

R = gas constant.

c_p = specific heat at constant pressure.

c_v = specific heat at constant volume.

γ = c_p/c_v.

e = internal energy per unit mass.

Q = heat added per unit mass.

μ_∞ = coefficient of viscosity at free stream temperature.

μ_o = coefficient of viscosity at stagnation temperature.

v = free stream velocity.

vn = velocity in boundary layer normal to surface.

vs = velocity in boundary layer parallel to surface.

vs_δ = vs at outermost edge of boundary layer.

$q_\infty = \frac{\gamma}{2} p_\infty M^2$ = free stream dynamic pressure.

Re = Reynold's number.

M = free stream Mach number.

τ = shearing stress at body surface.

D = skin friction drag.

C_D = skin friction drag coefficient.

$P(s) = 1 - (\frac{p}{po})^{\frac{\gamma - 1}{\gamma}}$.

$\lambda(\eta) = \frac{vs}{vs_\delta} = A\eta + B\eta^2 + C\eta^3 + \cdots\cdots$

$F1(s) = \int_o^1 \frac{2 P(s) \lambda(\eta)^2}{1 - P(s) \lambda(\eta)^2} d\eta$.

$F_2(s) = \int_o^1 \frac{\lambda(\eta) \sqrt{P(s)}}{1 - P(s) \lambda(\eta)^2} d\eta$.

C1 = $F_1(s)$ for zero pressure gradient.

C2 = F2(s) for zero pressure gradient.

$K_1 = \int_o^1 \lambda(\eta)^2 d\eta$

$K_2 = \int_o^1 \lambda(\eta) d\eta$

SECTION I

DEVELOPMENT OF INTEGRAL RELATIONS AND EXPRESSIONS FOR BOUNDARY LAYER THICKNESS

A. General Development

For the purpose of this analysis it is convenient to introduce an orthogonal, curvilinear, coordinate system defined as follows: (identical to that adopted in reference 6). Let x_1 = constant, x_2 = constant, x_3 = constant denote the three families of orthogonal surfaces defining the coordinate system. Then choose x_1 such that one member of the family x_1 = constant coincides with the boundary of the surface of revolution (cf. Figure 1). x_3 is chosen so that x_3 = constant gives planes through the axis of symmetry, i.e., x_3 is the azimuthal angle, θ , of Figure 1 then the surfaces x_2 = constant are perpendicular to the two other families. If ds is an element of length, then for such an orthogonal system we have in general

$$ds^2 = h_1^2 dx_1^2 + h_2^2 dx_2^2 + h_3^2 dx_3^2$$

where the coefficients h_1, h_2, h_3 are functions of x_1, x_2, x_3. Putting $dx_1 = dx_2 = 0$, it is seen that $h_3 = r$ where r is the distance of any point from the axis of symmetry. In this analysis interest is focused on the thin region, of thickness δ on either side of the boundary. If c_r denotes the "longitudinal" radius of curvature of the boundary and also if $\delta \ll c_r$; $h_1 = 1$, $h_2 = 1$.

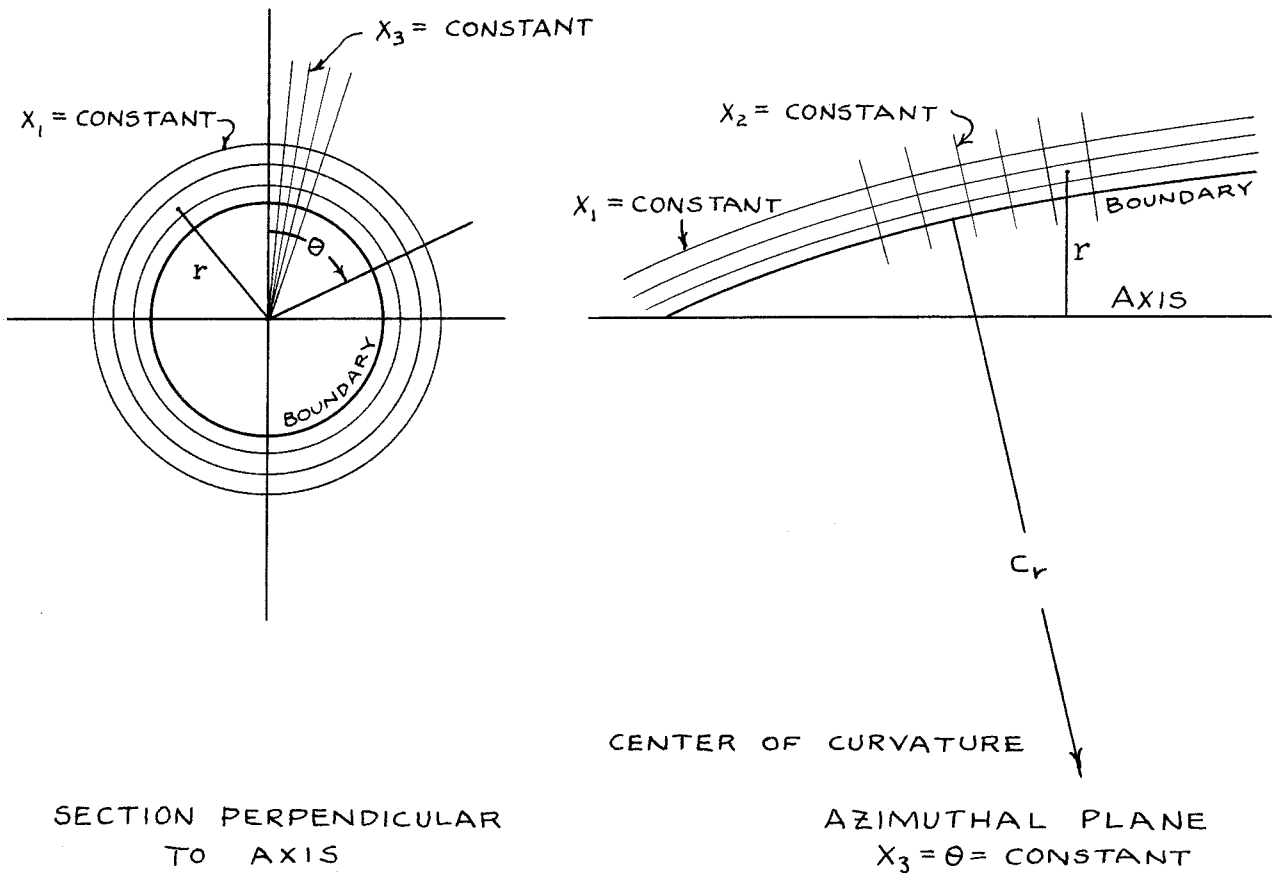

Figure 1 Coordinate System for A Figure of Revolution

Now choose the origin of x_1 at the boundary and that of x_2 at the most upstream point and write:

$x_1 = n$ = normal distance from the boundary

$x_2 = s$ = distance along boundary from the leading edge

Hence the curvilinear coordinate system is specified by:

$x_1 = n \quad h_1 = 1 \qquad\qquad n << c_r$

$x_2 = s \quad h_2 = 1$

$x_3 = \theta \quad h_3 = r(n,s)$

The velocity vector $\bar{q}$ is defined as

$$\bar{q} = v_n \bar{\iota}_n + v_s \bar{\iota}_s + v_\theta \bar{\iota}_\theta$$

where v_n, v_s, v_θ and $\bar{\iota}_n$, $\bar{\iota}_s$, $\bar{\iota}_\theta$ are the magnitudes of the velocity and the unit vector in th n, s, θ directions. From the assumption of axial symmetry, $\frac{\partial ( )}{\partial \theta} = v_\theta = 0$.

the basic equations of viscous compressible flow are the momentum equation: (references 7, 8)

$$\rho \frac{D\bar{q}}{Dt} = \rho g - \nabla p - \frac{2}{3} \nabla (\mu \nabla \cdot \bar{q}) + \nabla \cdot (\mu \phi) , \quad (1)$$

the continuity equation:

$$\nabla \rho \bar{q} + \frac{\partial \rho}{\partial t} = 0, \quad (2)$$

and the energy equation:

$$\rho \frac{D\bar{q}}{Dt} + \Phi = \rho \frac{De}{Dt} + \rho p \frac{D(\frac{1}{\rho})}{Dt} \quad (3)$$

Each of these equations will be expanded in turn and the notation will be explained in the expansion. Also the boundary layer assumptions will be applied to the expanded equations in the work that follows:

It should be noted that in general

$$\nabla A = \frac{1}{h_1} \frac{\partial A}{\partial x_1} \bar{\iota}_1 + \frac{1}{h_2} \frac{\partial A}{\partial x_2} \bar{\iota}_2 + \frac{1}{h_3} \frac{\partial A}{\partial x_3} \bar{\iota}_3 \quad \text{and}$$

$$\nabla \cdot \bar{A} = \frac{1}{h_1 h_2 h_3} \left[\frac{\partial}{\partial x_1} (h_2 h_3 A_1) + \frac{\partial}{\partial x_2} (h_3 h_1 A_2) + \frac{\partial}{\partial x_3} (h_1 h_2 A_3) \right]$$

In the present coordinate system the above reduces to

$$\nabla A = \frac{\partial A}{\partial n}\,\bar{\iota}_n + \frac{\partial A}{\partial s}\,\bar{\iota}_s$$

$$\text{and } \nabla\cdot\bar{A} = \frac{1}{r}\left[\frac{\partial}{\partial n}(rA_1) + \frac{\partial}{\partial s}(rA_2)\right]$$

Expansion of the momentum equation (1):

In equation (1) ρ is the density, $\frac{D(\ )}{D\,t}$ is the total derivative with respect to time, $\bar{q}$ is the velocity vector, g is the acceleration of gravity, p is the pressure, μ is the viscosity, $\phi = \nabla\bar{q} + (\nabla\bar{q})_{conj.}$, and ∇ is the vector operator, "gradient".

Consider the term $\nabla(\mu\nabla\cdot\bar{q})$

$$\nabla(\mu\nabla\cdot\bar{q}) = \nabla(AB) = A\nabla B + B\nabla A$$

$$B = \nabla\cdot\bar{q} = \frac{1}{r}\left[\frac{\partial}{\partial n}(rv_n) + \frac{\partial}{\partial s}(rv_s)\right]$$

$$\nabla B = \nabla(\nabla\cdot\bar{q}) = \frac{\partial}{\partial n}\left\{\frac{1}{r}\left[\frac{\partial}{\partial n}(rv_n) + \frac{\partial}{\partial s}(rv_s)\right]\right\}\bar{\iota}_n$$

$$\frac{\partial}{\partial s}\left\{\frac{1}{r}\left[\frac{\partial}{\partial n}(rv_n) + \frac{\partial}{\partial s}(rv_s)\right]\right\}\bar{\iota}_s$$

$$\nabla A = \frac{\partial\mu}{\partial n}\,\bar{\iota}_n + \frac{\partial\mu}{\partial s}\,\bar{\iota}_s$$

combining:

$$\nabla(\mu\nabla\cdot\bar{q}) = \mu\left[\frac{\partial}{\partial n}\left\{\frac{1}{r}\left[\frac{\partial}{\partial n}(rv_n) + \frac{\partial}{\partial s}(rv_s)\right]\right\}\bar{\iota}_n + \frac{\partial}{\partial s}\left\{\frac{1}{r}\left[\frac{\partial}{\partial n}(rv_n) + \frac{\partial}{\partial s}(rv_s)\right]\right\}\bar{\iota}_s\right]$$

$$+ \frac{1}{r}\left[\frac{\partial}{\partial n}(rv_n) + \frac{\partial}{\partial s}(rv_s)\right]\left[\frac{\partial\mu}{\partial n}\,\bar{\iota}_n + \frac{\partial\mu}{\partial s}\,\bar{\iota}_s\right] \qquad (1a)$$

Consider the term $\nabla\cdot(\mu\phi)$

$$\nabla\cdot(\mu\phi) = \nabla\mu\cdot\phi + \mu\nabla\cdot\phi$$

$$\phi = \nabla\bar{q} + (\nabla\bar{q})\text{conj.} = \bar{\imath}_n\frac{\partial\bar{q}}{\partial n} + \bar{\imath}_s\frac{\partial\bar{q}}{\partial s} + \frac{\partial\bar{q}}{\partial n}\bar{\imath}_n + \frac{\partial\bar{q}}{\partial s}\bar{\imath}_s$$

$$\nabla\cdot\phi = (\nabla\cdot\bar{\imath}_n)\frac{\partial\bar{q}}{\partial n} + (\nabla\cdot\bar{\imath}_s)\frac{\partial\bar{q}}{\partial s} + (\nabla\cdot\frac{\partial\bar{q}}{\partial n})\bar{\imath}_n + (\nabla\cdot\frac{\partial\bar{q}}{\partial s})\bar{\imath}_s$$

After expansion the term becomes:

$$\nabla\cdot(\mu\phi) = \mu\left[\frac{\partial^2 v_n}{\partial n^2}\bar{\imath}_n + \frac{\partial^2 v_s}{\partial n^2}\bar{\imath}_s + \frac{\partial^2 v_n}{\partial s^2}\bar{\imath}_n + \frac{\partial^2 v_s}{\partial s^2}\bar{\imath}_s + \frac{\partial^2 v_n}{\partial n^2}\bar{\imath}_n + \frac{\partial^2 v_s}{\partial s\partial n}\bar{\imath}_n + \frac{\partial^2 v_n}{\partial n\partial s}\bar{\imath}_s + \frac{\partial^2 v_s}{\partial s^2}\bar{\imath}_s\right]$$

$$+ \frac{\partial\mu}{\partial n}\frac{\partial v_n}{\partial n}\bar{\imath}_n + \frac{\partial\mu}{\partial n}\frac{\partial v_s}{\partial n}\bar{\imath}_s + \frac{\partial\mu}{\partial s}\frac{\partial v_n}{\partial s}\bar{\imath}_n + \frac{\partial\mu}{\partial s}\frac{\partial v_s}{\partial s}\bar{\imath}_s$$

$$+ \frac{\partial\mu}{\partial n}\frac{\partial v_n}{\partial n}\bar{\imath}_n + \frac{\partial\mu}{\partial n}\frac{\partial v_n}{\partial s}\bar{\imath}_s + \frac{\partial\mu}{\partial s}\frac{\partial v_s}{\partial n}\bar{\imath}_n + \frac{\partial\mu}{\partial s}\frac{\partial v_s}{\partial s}\bar{\imath}_s \qquad (1b)$$

Consider the term $\frac{D\bar{q}}{Dt}$

$$\frac{D\bar{q}}{Dt} = \left[\frac{\partial v_n}{\partial t} + v_n\frac{\partial v_n}{\partial n} + v_s\frac{\partial v_n}{\partial s}\right]\bar{\imath}_n + \left[\frac{\partial v_s}{\partial t} + v_n\frac{\partial v_s}{\partial t} + v_s\frac{\partial v_s}{\partial t}\right]\bar{\imath}_s \qquad (1c)$$

the term $\nabla p = \frac{\partial p}{\partial s}\bar{\imath}_s + \frac{\partial p}{\partial n}\bar{\imath}_n$ (1d)

Gravity is neglected; therefore the gravity term = 0. (1e)

Combining the $\bar{\imath}_n$ terms in equations (1a) through (1e),

$$\rho\left[\frac{\partial v_n}{\partial t}+v_n\frac{\partial v_n}{\partial n}+v_s\frac{\partial v_n}{\partial s}\right]=-\frac{\partial p}{\partial n}+$$

$$-\frac{2}{3}\left[\mu\left[\frac{\partial}{\partial n}\left[\frac{1}{r}\left\{\frac{\partial}{\partial n}(rv_n)+\frac{\partial}{\partial s}(rv_s)\right\}\right]\right]+\frac{\partial\mu}{\partial n}\left[\frac{1}{r}\left[\frac{\partial}{\partial n}(rv_n)+\frac{\partial}{\partial s}(rv_s)\right]\right]\right]$$

$$+\mu\left[2\frac{\partial^2 v_n}{\partial n^2}+\frac{\partial^2 v_s}{\partial s\,\partial n}+\frac{\partial^2 v_n}{\partial s^2}\right]+2\frac{\partial\mu}{\partial n}\frac{\partial v_n}{\partial n}+\frac{\partial\mu}{\partial s}\frac{\partial v_n}{\partial s}\quad\frac{\partial\mu}{\partial s}\frac{\partial v_s}{\partial n}$$

(1f)

Combining the $\bar{\iota}_s$ terms in equations (1a) thru (1e)

$$\rho\left[\frac{\partial v_s}{\partial t}+v_n\frac{\partial v_s}{\partial n}+v_s\frac{\partial v_s}{\partial s}\right]=-\frac{\partial p}{\partial s}+$$

$$-\frac{2}{3}\left[\mu\left[\frac{\partial}{\partial s}\left[\frac{1}{r}\left\{\frac{\partial}{\partial n}(rv_n)+\frac{\partial}{\partial s}(rv_s)\right\}\right]\right]+\frac{\partial\mu}{\partial s}\left[\frac{1}{r}\left[\frac{\partial}{\partial n}(rv_n)+\frac{\partial}{\partial s}(rv_s)\right]\right]\right]$$

$$+\mu\left[2\frac{\partial^2 v_s}{\partial s^2}+\frac{\partial^2 v_n}{\partial n\,\partial s}+\frac{\partial^2 v_s}{\partial n^2}\right]+2\frac{\partial\mu}{\partial s}\frac{\partial v_s}{\partial s}+\frac{\partial\mu}{\partial n}\frac{\partial v_s}{\partial n}+\frac{\partial\mu}{\partial n}\frac{\partial v_n}{\partial s}$$

(1g)

It is now assumed that v_n is a small fraction of v_s and that the range of n in the boundary layer is small compared to distance along the boundary layer. It is convenient to write $n=\epsilon\eta$ and $v_n=\epsilon\bar{v}$ where ϵ is a small quantity compared to unity and η and $\bar{v}$ are comparable to s and v_s respectively. The boundary layer equations are deduced on the basis that terms of the lowest order in ϵ are to be retained. Introducing these concepts into equation (1g), the

following is obtained:

$$\rho \frac{\partial v_s}{\partial t} + \rho \frac{\varepsilon}{\varepsilon} \bar{v} \frac{\partial v_s}{\partial \eta} + \rho v_s \frac{\partial v_s}{\partial s} = -\frac{\partial p}{\partial s} - \frac{2}{3}\mu \frac{\partial}{\partial s}\left[\frac{\varepsilon}{\varepsilon}\frac{\partial \bar{v}}{\partial \eta} + \frac{\varepsilon \bar{v}}{r}\frac{1}{\varepsilon}\frac{\partial r}{\partial \eta} + \frac{v_s}{r}\frac{\partial v_s}{\partial s} + \frac{\partial v_s}{\partial s}\right]$$

$$- \frac{2}{3}\frac{\partial \mu}{\partial s}\left[\frac{\varepsilon}{\varepsilon}\frac{\partial \bar{v}}{\partial \eta} + \frac{\varepsilon}{r}\frac{\bar{v}}{\varepsilon}\frac{\partial r}{\partial \eta} + \frac{\partial v_s}{\partial s} + \frac{v_s}{r}\frac{\partial r}{\partial s}\right] + 2\mu \frac{\partial^2 v_s}{\partial s^2} + \mu \frac{\varepsilon}{\varepsilon}\frac{\partial^2 \bar{v}}{\partial \eta \partial s}$$

$$+ \frac{\mu}{\varepsilon^2}\frac{\partial^2 v_s}{\partial \eta^2} + 2\frac{\partial \mu}{\partial s}\frac{\partial v_s}{\partial s} + \frac{1}{\varepsilon^2}\frac{\partial \mu}{\partial \eta}\frac{\partial v_s}{\partial \eta} + \frac{1}{\varepsilon}\frac{\partial \mu}{\partial \eta}\varepsilon\frac{\partial \bar{v}}{\partial s} \qquad (1h)$$

The most important power of ε is -2 and occurs in the above equation in association with μ and $\frac{\partial \mu}{\partial \eta}$. In the boundary layer equations it is assumed that the terms $\frac{\mu}{\varepsilon^2}\frac{\partial^2 v_s}{\partial \eta^2}$ and $\frac{1}{\varepsilon^2}\frac{\partial \mu}{\partial \eta}\frac{\partial v_s}{\partial \eta}$ are of the same importance as $\rho v_s \frac{\partial v_s}{\partial s}$ and other terms not involving ε. Since $\frac{\partial^2 v_s}{\partial \eta^2}$ is itself of zero order in ε, the hypothesis is equivalent to assuming μ a small quantity in the second order of ε. Neglecting the less important terms equation (1h) becomes

$$\rho \frac{\partial v_s}{\partial t} + \rho \bar{v} \frac{\partial v_s}{\partial \eta} + \rho v_s \frac{\partial v_s}{\partial s} = -\frac{\partial p}{\partial s} + \frac{\mu}{\varepsilon^2}\frac{\partial^2 v_s}{\partial \eta^2} + \frac{1}{\varepsilon^2}\frac{\partial \mu}{\partial \eta}\frac{\partial v_s}{\partial \eta} \qquad (1i)$$

In a similar manner (1f) becomes:

$$\rho\varepsilon \frac{\partial \bar{v}}{\partial t} + \rho \frac{\varepsilon^2}{\varepsilon}\frac{\partial \bar{v}}{\partial \eta} + \rho v_s \varepsilon \frac{\partial \bar{v}}{\partial s} = -\frac{1}{\varepsilon}\frac{\partial p}{\partial \eta} +$$

$$- \frac{2}{3}\frac{\mu}{\varepsilon}\frac{\partial}{\partial \eta}\left[\frac{\varepsilon}{\varepsilon}\frac{\partial \bar{v}}{\partial \eta} + \frac{\varepsilon}{r}\frac{\bar{v}}{\varepsilon}\frac{1}{\varepsilon}\frac{\partial r}{\partial \eta} + \frac{\partial v_s}{\partial s} + \frac{v_s}{r}\frac{\partial r}{\partial s}\right] +$$

$$- \frac{2}{3\varepsilon}\frac{\partial \mu}{\partial \eta}\left[\frac{\varepsilon}{\varepsilon}\frac{\partial \bar{v}}{\partial \eta} + \frac{\varepsilon}{r}\frac{\bar{v}}{\varepsilon}\frac{\partial r}{\partial \eta} + \frac{\partial v_s}{\partial s} + \frac{v_s}{r}\frac{\partial r}{\partial s}\right] + 2\mu\frac{\varepsilon}{\varepsilon^2}\frac{\partial^2 \bar{v}}{\partial \eta^2}$$

$$+ \frac{\mu}{\varepsilon}\frac{\partial^2 v_s}{\partial s \partial \eta} + \mu\varepsilon\frac{\partial^2 \bar{v}}{\partial s^2} + 2\frac{\varepsilon}{\varepsilon^2}\frac{\partial \mu}{\partial \eta}\frac{\partial \bar{v}}{\partial \eta} + \frac{\partial \mu}{\partial s}\varepsilon\frac{\partial \bar{v}}{\partial s} + \frac{1}{\varepsilon}\frac{\partial \mu}{\partial s}\frac{\partial v_s}{\partial \eta} \qquad (1j)$$

Now noting that μ , $\frac{\partial \mu}{\partial \eta}$, and $\frac{\partial \mu}{\partial s}$ are of the order ε^2, it is seen that the lowest ordered term in equation (1j) is that of order ε . Consequently $\frac{1}{\varepsilon}\frac{\partial p}{\partial \eta}$ can be of no lower order than that of ε . Hence $\frac{\partial p}{\partial \eta}$ is at best of the order ε^2 and it may safely be assumed that there is no change in pressure normal to the surface through the boundary layer.

Assuming steady state conditions the approximate momentum equation for the boundary layer becomes (transforming equation (1i) back to dimensional coordinates).

$$\rho v_n \frac{\partial v_s}{\partial n} + \rho v_s \frac{\partial v_s}{\partial s} = -\frac{dp}{ds} + \frac{\partial}{\partial n}\left(\mu \frac{\partial v_s}{\partial n}\right) \qquad (4)$$

Expansion of the continuity equation (2) :

Assuming steady state equation (2) reduces immediately to

$$\frac{\partial}{\partial n}(r\rho v_n) + \frac{\partial}{\partial s}(r\rho v_s) = 0 \qquad (5)$$

Expansion of the energy equation (3) :

$$\rho \frac{DQ}{Dt} + \Phi = \frac{De}{Dt} + \rho p \frac{D(\frac{1}{\rho})}{Dt} \qquad (3)$$

In this equation Q is the heat added per unit mass by conduction

Φ is the dissipation function defined below

e is the internal energy per unit mass

$P \frac{D(\frac{1}{\rho})}{Dt}$ is the work done by a fluid element by expansion

$$\Phi = \tau_{nn} \frac{\partial v_n}{\partial n} + \tau_{sn} \left(\frac{\partial v_s}{\partial n} + \frac{\partial v_n}{\partial s} \right) + \tau_{ss} \frac{\partial v_s}{\partial s} \qquad (3a)$$

where τ_{xy} are stress tensors defined as follows:

$$\begin{Bmatrix} \tau_{nn} & \tau_{ns} \\ \tau_{sn} & \tau_{ss} \end{Bmatrix} = \mu \begin{Bmatrix} \frac{\partial v_n}{\partial n} & \frac{\partial v_s}{\partial n} \\ \frac{\partial v_n}{\partial s} & \frac{\partial v_s}{\partial s} \end{Bmatrix} + \mu \begin{Bmatrix} \frac{\partial v_n}{\partial n} & \frac{\partial v_n}{\partial s} \\ \frac{\partial v_s}{\partial n} & \frac{\partial v_s}{\partial s} \end{Bmatrix} - \begin{Bmatrix} p & 0 \\ 0 & p \end{Bmatrix} - \frac{2}{3}\mu \begin{Bmatrix} \nabla\cdot\bar{q} & 0 \\ 0 & \nabla\cdot\bar{q} \end{Bmatrix}$$

thus

$$\left.\begin{aligned} \tau_{nn} &= 2\mu \frac{\partial v_n}{\partial n} - p - \frac{2}{3}\mu \nabla\cdot\bar{q} \\ \tau_{sn} &= \tau_{ns} = \mu \frac{\partial v_s}{\partial n} + \mu \frac{\partial v_n}{\partial s} \\ \tau_{ss} &= 2\mu \frac{\partial v_s}{\partial s} - p - \frac{2}{3}\mu \nabla\cdot\bar{q} \end{aligned}\right\} \qquad (3b)$$

the first term on the left hand side of equation (3) is

$$\rho \frac{DQ}{Dt} = \frac{\partial}{\partial n}\left(k \frac{\partial T}{\partial n} \right) + \frac{\partial}{\partial s}\left(k \frac{\partial T}{\partial s} \right) \qquad (3c)$$

where k is the heat conduction coefficient and T is the absolute temperature.

The right hand side of the equation may be written as

$$\rho\left[\frac{De}{Dt} + p\,\frac{D(\frac{1}{\rho})}{Dt}\right] = \rho\,\frac{D}{Dt}\,(e+\frac{p}{\rho}) - \frac{Dp}{Dt} = \rho\,\frac{D(C_p T)}{Dt} - \frac{Dp}{Dt} \qquad (3d)$$

since $e + \frac{p}{\rho}$ = enthalpy per unit mass = $C_p T$.

Inserting equations (3a) through (3d) into (3) there is obtained:

$$\frac{\partial}{\partial n}\,(k\,\frac{\partial T}{\partial n}) + \frac{\partial}{\partial s}\,(k\,\frac{\partial T}{\partial s}) + (2\mu\,\frac{\partial v_n}{\partial n} - p - \frac{2}{3}\mu\,\nabla\cdot\bar{q})\,\frac{\partial v_n}{\partial n}$$

$$+ (\mu\,\frac{\partial v_s}{\partial n} + \mu\,\frac{\partial v_n}{\partial s})\,(\frac{\partial v_s}{\partial n} + \frac{\partial v_n}{\partial s}) \quad (2\mu\,\frac{\partial v_s}{\partial s} - p - \frac{2}{3}\mu\,\nabla\cdot\bar{q})\,\frac{\partial v_s}{\partial s}$$

$$= \frac{D(C_p T)}{Dt} - \frac{Dp}{Dt} \qquad (3e)$$

Upon introduction of ε, η, $\bar{v}$, equation (3e) becomes:

$$\frac{1}{\varepsilon^2}\,\frac{\partial}{\partial \eta}\,(k\,\frac{\partial T}{\partial \eta}) + \frac{\partial}{\partial s}\,(k\,\frac{\partial T}{\partial s}) + \left[2\mu\,\frac{\varepsilon}{\varepsilon}\,\frac{\partial \bar{v}}{\partial \eta} - p - \frac{2}{3}\mu\,(\frac{\varepsilon}{\varepsilon}\,\frac{\partial \bar{v}}{\partial \eta} + \frac{\partial v_s}{\partial s})\right]\frac{\varepsilon}{\varepsilon}\,\frac{\partial \bar{v}}{\partial \eta}$$

$$+ (\mu\,\frac{1}{\varepsilon}\,\frac{\partial v_s}{\partial \eta} + \mu\,\varepsilon\,\frac{\partial \bar{v}}{\partial s}) \quad (\frac{1}{\varepsilon}\,\frac{\partial v_s}{\partial \eta} + \varepsilon\,\frac{\partial \bar{v}}{\partial s})$$

$$+ \left[2\mu\,\frac{\partial v_s}{\partial s} - p - \frac{2}{3}\mu\,(\frac{\varepsilon}{\varepsilon}\,\frac{\partial \bar{v}}{\partial \eta} + \frac{\partial v_s}{\partial s})\right]\frac{\partial v_s}{\partial s}$$

$$= \rho\,\frac{\partial C_p T}{\partial t} + \rho\,\frac{\varepsilon}{\varepsilon}\,\bar{v}\,\frac{\partial C_p T}{\partial \eta} + \rho\,v_s\,\frac{\partial C_p T}{\partial s} - (\frac{\partial p}{\partial t} + \frac{\varepsilon}{\varepsilon}\,\bar{v}\,\frac{\partial p}{\partial \eta} + v_s\,\frac{\partial p}{\partial s}) \qquad (3f)$$

Considering now that μ, k are of second order $\sim \varepsilon^2$, steady state conditions, and remembering that $\frac{\partial p}{\partial \eta} \doteq 0$ from the momentum equation, equation (3f) for steady flow reduces to:

$$\frac{1}{\varepsilon^2}\frac{\partial}{\partial\eta}\left(k\frac{\partial T}{\partial\eta}\right)+\frac{\mu}{\varepsilon^2}\left(\frac{\partial v_s}{\partial\eta}\right)^2 = \rho\bar{v}\frac{\partial C_pT}{\partial\eta}+\rho v_s\frac{\partial C_pT}{\partial s}-v_s\frac{\partial p}{\partial s} \qquad (3g)$$

transforming to dimensional coordinates equation (3g) becomes

$$\frac{\partial}{\partial n}\left(k\frac{\partial T}{\partial n}\right)+\mu\left(\frac{\partial v_s}{\partial n}\right)^2 = \rho v_n\frac{\partial CpT}{\partial n}+\rho v_s\frac{\partial CpT}{\partial s}-v_s\frac{\partial p}{\partial s} \qquad (6)$$

A solution to the above equation for the particular assumption that there is no heat transfer through the surface, (Prandtl Number $\sigma = 1$), and C_p = constant, is

$$C_pT+v_s^2 = C_pT_o \qquad \text{(reference 8)} \qquad (7)$$

Equations (4), (5), (7) are now applied to four specific cases as listed below:

Case I Compressible flow with a pressure gradient

Case II Compressible flow with no pressure gradient

Case III Incompressible flow with a pressure gradient

Case IV Incompressible flow with no pressure gradient

B.

Case I Compressible Flow with Pressure Gradient

Consider the momentum equation (4)

$$\rho v_n\frac{\partial v_s}{\partial n}+\rho v_s\frac{\partial v_s}{\partial s} = -\frac{dp}{ds}+\frac{\partial}{\partial n}\left(\mu\frac{\partial v_s}{\partial n}\right) \qquad (4)$$

and the continuity equation (5)

$$\frac{\partial}{\partial n}(r\rho v_n)+\frac{\partial}{\partial s}(r\rho v_s) = 0 \qquad (5)$$

Multiply the momentum equation by $r\,dn$ and integrate from 0 to δ where δ is the boundary layer thickness.

$$\int_0^{\delta} \rho\, r\, v_n \frac{\partial v_s}{\partial n}\, dn + \int_0^{\delta} \rho\, r\, v_s \frac{v_s}{s}\, dn = -\int_0^{\delta} r \frac{dp}{ds} + \int_0^{\delta} r \frac{\partial}{\partial n}\left(\mu \frac{\partial v_s}{\partial n}\right) dn \qquad (4a)$$

Consider the first term on the L.H.S. of equation (4a). By partial integration this term becomes:

$$\int_0^{\delta} \rho\, r\, v_n \frac{\partial v_s}{\partial n}\, dn = \rho\, r v_n\, v_s \Big|_0^{\delta} - \int_0^{\delta} v_s \frac{\partial (\rho\, r\, v_n)}{\partial n}\, dn \qquad (4b)$$

However at $n = 0$, $v_s = 0$, and from the continuity equation (5)

$$\frac{\partial (\rho\, r v_n)}{\partial n} = -\frac{\partial (\rho\, r v_s)}{\partial s}$$

then equation (4b) becomes:

$$\int_0^{\delta} \rho\, r\, v_n \frac{\partial v_s}{\partial n}\, dn = \rho_\delta\, r_\delta\, v_{n_\delta}\, v_{s_\delta} + \int_0^{\delta} v_s \frac{\partial (\rho\, r v_s)}{\partial s}\, dn \qquad (4c)$$

where the subscript δ signifies values of the quantities at $n = \delta$.

Inserting (4c) into (4a),

$$\rho_\delta\, r_\delta\, v_{n_\delta}\, v_{s_\delta} + \int_0^{\delta} \left[\rho\, r\, v_s \frac{\partial v_s}{\partial s} + v_s \frac{\partial (\rho\, r v_s)}{\partial s}\right] dn$$

$$= -\int_0^{\delta} r\, dn + \int_0^{\delta} r \frac{\partial}{\partial n}\left(\mu \frac{\partial v_s}{\partial n}\right) dn \qquad (4d)$$

The integral term on the L.H.S. of equation (4d) may be written as

$$\int_0^{\delta} \frac{\partial (\rho\, r v_s^2)}{\partial s}\, dn$$

However $$\int_0^\delta \frac{\partial(\rho r v_s^2)}{\partial s}\, dn = \frac{d}{ds}\int_0^\delta \rho r v_s^2 dn - \rho_\delta r_\delta v_{s_\delta}^2 \frac{d\delta}{ds} \qquad (4e)$$

Consequently the acceleration terms in the momentum equation reduce to:

$$\rho_\delta r_\delta v_{n_\delta} v_{s_\delta} + \frac{d}{ds}\int_0^\delta \rho r v_s^2 dn - \rho_\delta r_\delta v_{s_\delta}^2 \frac{d\delta}{ds} \qquad (4f)$$

Now to reduce these terms to an integral form, consider:

$$-\rho_\delta r_\delta v_{s_\delta} \frac{d\delta}{ds} = -\frac{d}{ds}\int_0^\delta \rho r v_s\, dn + \int_0^\delta \frac{\partial}{\partial s}(\rho r v_s)\, dn \qquad (4g)$$

But by virtue of the continuity equation (5)

$$\frac{\partial}{\partial s}(\rho r v_s) = -\frac{\partial}{\partial n}(\rho r v_n)$$

then $$\int_0^\delta \frac{\partial}{\partial s}(\rho r v_s)\, dn = -\int_0^\delta \frac{\partial}{\partial n}(\rho r v_n)\, dn = -\rho_\delta r_\delta v_{n_\delta} \qquad (4h)$$

Multiply (4h) by v_{s_δ} :

$$-\rho_\delta r_\delta v_{s_\delta}^2 \frac{d\delta}{ds} = -v_{s_\delta}\frac{d}{ds}\int_0^\delta \rho r v_s\, dn - \rho_\delta r_\delta v_{n_\delta} v_{s_\delta} \qquad (4i)$$

Now inserting (4i) into (4f) the acceleration terms become:

$$\frac{d}{ds}\int_0^\delta \rho r v_s^2\, dn - v_{s_\delta}\frac{d}{ds}\int_0^\delta \rho r v_s\, dn \qquad (4j)$$

Inserting (4i) into (4a) the integral momentum equation is:

$$\frac{d}{ds}\int_0^\delta \rho r v_s^2 dn - v_{s_\delta}\frac{d}{ds}\int_0^\delta \rho r v_s\, dn = -\int_0^\delta r\frac{dp}{ds} + \int_0^\delta r\frac{\partial}{\partial n}\left(\mu\frac{\partial v_s}{\partial n}\right) dn \qquad (8)$$

Equation (8) is completely valid within the limitations imposed by the conditions of axial symmetry and the usual boundary layer approximations. Now however, assuming no heat transfer through the boundary and the equation of state for a perfect gas ($p = \rho RT$), equation (7) may be used to give an expression for the density of the fluid in the boundary layer as a function of (p, T, v_s).

$$\rho = \frac{p}{RT}$$

and from equation (7) $\quad T = \frac{1}{C_p}\left(C_pT_o - \frac{1}{2}\, v_s^2\right)$,

and using $\frac{C_p}{R} = \frac{C_p}{C_p - C_v} = \frac{\gamma}{\gamma - 1}$, it is found that

$$\rho = \frac{\gamma}{\gamma - 1}\, \frac{p}{\left(C_pT_o - \frac{v_s^2}{2}\right)} \tag{9}$$

Assume that the radial distance from the axis of symmetry to any point in the boundary layer equals the radial distance to the boundary

$(r \doteq r_o)$ (10)

Assume a cubic form of velocity profile in the boundary layer

(see Section III) $\quad v_s = A\eta + B\eta^2 + C\eta^3$ (11)

where $\quad \eta = \frac{n}{\delta}$ (11a)

the boundary conditions to be satisfied are the following:

at $\eta = 1 \quad v_s = v_{s_\delta} \quad \frac{\partial v_s}{\partial \eta} = 0 \quad \frac{\partial^2 v_s}{\partial \eta^2} = 0$

at $\eta = 0$ $\qquad v_s = 0.$

these conditions reduce equation (11) to

$$v_s = v_{s_\delta} (3\eta - 3\eta^2 + \eta^3) \tag{12}$$

Introducing equations (9), (10) in equation (8), noting that

$$\int_o^\delta r_o \frac{\partial}{\partial n} (\mu \frac{\partial v_s}{\partial n}) \, dn = - r_o \mu_o (\frac{\partial v_s}{\partial n})_{n = o}$$ since

$\frac{\partial v_s}{\partial n} = 0$ at $n = \delta$, and changing the variable of integration from n to η according to equation (11a), equation (8) becomes:

$$\frac{\gamma}{\gamma - 1} \frac{d}{ds} \left[r_o \, p \delta \int_o^1 \frac{v_s^2}{C_p T_o - \frac{v_s^2}{2}} \, d\eta \right] - \frac{\gamma}{\gamma - 1} v_{s_\delta} \frac{d}{ds} \left[r_o \, p \delta \int_o^1 \frac{v_s}{C_p T_o - \frac{v_s^2}{2}} \, d\eta \right]$$

$$= - \frac{dp}{ds} r_o \delta \int_o^1 d\eta - \frac{r_o \mu_o}{\delta} (\frac{\partial v_s}{\partial \eta})_{\eta = o} \tag{13}$$

Determination of v_{s_δ}

Again making use of equation (8)

$$v_s = \sqrt{2 C_p T_o (1 - \frac{T}{T_o})} \tag{14}$$

In the case under consideration v_{s_δ} is the velocity along the outer edge of the boundary layer and is in a region of flow which is beyond a shock wave. Consequently the ratio $\frac{T}{T_o}$ is dependent on the

ratio of the static pressure to the stagnation pressure after shock, P_o'. However, Table I which presents data obtained from reference 9 indicates that an assumption of $P_o/P_o' = 1$ is justifiable for the specific examples to be considered.

Consequently, assuming an isentropic expansion beyond the shock equation (14) may be written as:

$$v_{s_\delta} = \sqrt{2\, C_p T_o \left[1 - \left(\frac{p}{p_o}\right)^{\frac{\gamma-1}{\gamma}}\right]} \qquad (14a)$$

Of course for subsonic compressible flow the identical relation (14a) may be employed.

Consider the term $\int_o^1 \frac{v_s^2}{C_p T_o - \frac{v_s^2}{2}}\, d\eta$ of equation (13)

Introducing equation (12) and (14a) into the above term,

$$\int_o^1 \frac{v_s^2}{C_p T_o - \frac{v_s^2}{2}}\, d\eta = \int_o^1 \frac{2\, C_p T_o \left[1 - \left(\frac{p}{p_o}\right)^{\frac{\gamma-1}{\gamma}}\right] (3\eta - 3\eta^2 + \eta^3)^2}{C_p T_o - C_p T_o \left[1 - \left(\frac{p}{p_o}\right)^{\frac{\gamma-1}{\gamma}}\right](3\eta - 3\eta^2 + \eta^3)^2}\, d\eta \qquad (13a)$$

call $1 - \left(\frac{p}{p_o}\right)^{\frac{\gamma-1}{\gamma}} = P(s)$

$3\eta - 3\eta^2 + \eta^3 = \lambda(\eta)$

the term becomes $\int_o^1 \frac{2\, P(s)\, \lambda(\eta)^2}{1 - P(s)\lambda(\eta)^2}\, d\eta$

For a given pressure distribution this term may readily be integrated to give $F_1(s)$ (13b)

In a like manner the term $\int_0^1 \frac{v_s}{C_p T_o - \frac{v_s^2}{2}} \, d\eta$ (13c)

of equation (13) may be integrated for the given pressure distribution

to give $\sqrt{\frac{2}{C_p T_o}} \; F_2 (s)$ (13d)

the term $\int_0^1 d\eta$ becomes 1 (13e)

the term $\left(\frac{\partial v_s}{\partial \eta}\right)_{\eta = o}$ becomes simply $3 v_{s_\delta}$ (13f)

by inspection of equation (12).

TABLE I

RATIO OF STAGNATION PRESSURE AFTER SHOCK TO STAGNATION PRESSURE BEFORE SHOCK VS. MACH NUMBER AT INFINITY

(REFERENCE 9)

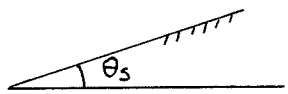

For $\theta_s = 10^\circ$

M_∞	P_o'/P_o
1.39	1.000
1.81	1.000
2.39	1.000
3.33	0.992
5.46	0.946

For $\theta_s = 20^\circ$

M_∞	P_o'/P_o
1.30	0.999
1.65	0.998
2.13	0.987
2.87	0.945
4.17	0.791
9.74	0.170

Now inserting equations (13b) through (13f) into equation (13),

$$\frac{\gamma}{\gamma-1}\frac{d}{ds}\left[r_o\, p\delta F_1(s)\right] - \frac{\gamma}{\gamma-1} v_{s_\delta}\frac{d}{ds}\left[r_o\, p\delta\, \frac{2}{C_pT_o} F_2(s)\right] = \tag{15}$$

$$-\frac{dp}{ds} r_o\delta - \frac{3r_o\mu_o}{\delta} v_{s_\delta}$$

Upon expansion of the L.H.S of equation (15) and dividing through by the coefficient of $\frac{d\delta}{ds}$, the equation becomes:

$$\frac{d\delta}{ds} + \frac{\delta\left[\frac{d}{ds}(r_o\, pF_1) - v_{s_\delta}\sqrt{\frac{2}{C_pT_o}}\frac{d}{ds}(r_o\, p\, F_2) + \frac{\gamma-1}{\gamma} r_o\frac{dp}{ds}\right]}{r_o\, p\left[F_1 - v_{s_\delta}\sqrt{\frac{2}{C_pT_o}}\, F_2\right]}$$

$$= -\frac{3\ \mu_o\ v_{s_\delta}}{\delta\ \frac{\gamma}{\gamma-1} P\left[F_1 - v_{s_\delta}\sqrt{\frac{2}{C_pT_o}}\ F_2\right]} \tag{15a}$$

Now multiplying the equation by δ and noting that

$$\delta\frac{d\delta}{ds} = \frac{1}{2}\frac{d\delta^2}{ds}$$ the equation (15a) becomes:

$$\frac{d\delta^2}{ds} + \delta^2\frac{\left[\frac{d}{ds}(r_o p\, F_1) - v_{s_\delta}\sqrt{\frac{2}{C_pT_o}}\ \frac{d}{ds}(r_o p\, F_2) + \frac{\gamma-1}{\gamma} r_o\frac{dp}{ds}\right]}{\frac{1}{2} r_o\, p\left[F_1 - v_{s_\delta}\sqrt{\frac{2}{C_pT_o}}\ F_2\right]} =$$

$$-\frac{3\ \mu_o\ v_{s_\delta}}{\frac{1}{2}\frac{\gamma}{\gamma-1}\ p\left[F_1 - v_{s_\delta}\sqrt{\frac{2}{C_pT_o}}\ F_2\right]} \tag{16}$$

Equation (16) is the differential equation for the thickness

of the boundary layer in compressible flow with a pressure gradient as a function of the distance along the boundary. Although the equation is of the form

$$\frac{dy}{ds} + G(s)\, y = H(s) \tag{16a}$$

it is not amenable to direct integration because of the complexity of the functions $G(s)$ and $H(s)$. The evaluation of δ^2 is accomplished by a numerical method of integration as will be shown under the computation section.

C.

Case II Compressible Flow with No Pressure Gradient

This case is identical to Case I with the following exceptions:

$$\frac{dP}{ds} = 0 \qquad \text{in equation (13)}$$

and the terms $F_1(s)$, $F_2(s)$, of (13a), (13b) and v_{s_δ} are now constant with respect to s.

Equation (16) reduces immediately to the following:

$$\frac{d\delta^2}{ds} + \delta^2 \frac{d(\log r_o^2)}{ds} = \frac{-6 \mu_o v_{s_\delta}}{\frac{\gamma}{\gamma - 1} P\left(C_1 - v_{s_\delta}\sqrt{\frac{2}{C_p T_o}}\, C_2\right)} \tag{17}$$

For a given v_{s_δ} and p, equation (17) may be written as

$$\frac{d\delta^2}{ds} + \delta^2 \frac{d(\log r_o^2)}{ds} = K \tag{17a}$$

where K is a constant.

The solution of (17a) follows directly:

$$\delta^2 = e^{-\int \frac{d(\log r_o^2)}{ds} ds} K \int_o^s e^{\int \frac{d \log r_o^2}{ds} ds} ds \qquad (17b)$$

However

$$e^{-\int \frac{d \log r_o^2}{ds} ds} = e^{-\log r_o^2} = \frac{1}{r_o^2}$$

and

$$e^{\int \frac{d \log r_o^2 ds}{ds}} = e^{\log r_o^2} = r_o^2$$

then

$$\delta^2 = K \frac{\int_o^s r_o^2 \, ds}{r_o^2} \qquad (17c)$$

Equation (17c) is valid if $\frac{\int_o^s r_o^2 \, ds}{r_o^2}$ remains finite as s approaches zero. To evaluate the limit of this expression as s approaches zero, consider that the axial symmetric body can be approximated by a cone in the neighborhood of $s \longrightarrow 0$. That is, assume $r_o = k s$

$$\int r_o^2 ds = \int k^2 s^2 ds = \frac{k^2 s^3}{3}$$

then

$$\frac{\int r_o^2 \, ds}{r_o^2} \longrightarrow \frac{\frac{k^2 s^3}{3}}{k^2 s^2} = \frac{s}{3}$$

As $s \longrightarrow 0$, $\frac{\int r_o^2 \, ds}{r_o^2} \longrightarrow 0$ faster, and equation (17c) is valid.

The equation for δ^2 in Case II is then:

$$\delta^2 = \frac{-6\mu_o v_{s_\delta}}{\frac{\gamma}{\gamma-1} P \left(C_1 - v_{s_\delta}\sqrt{\frac{2}{C_pT_o}}\, C_2\right)} \frac{\int_o^s r_o^2\, ds}{r_o^2} \qquad (18)$$

From an examination of equation (18) it appears that for Case II, the shape of boundary layer thickness is uniquely determined by the geometry of the body, and the magnitude of the thickness is determined by the value of the constant K of equation (17c).

D.

Case III Incompressible Flow with Pressure Gradient

For this case the differential relation follows immediately from equation (13) under Case I.

$$\frac{d}{ds}\left[r_o\delta\int_o^1 v_s^2 d\eta\right] - v_{s_\delta}\frac{d}{ds}\left[r_o\delta\int_o^1 v_s d\eta\right] = -\frac{r_o}{\rho}\frac{dp}{ds}\delta\int_o^1 d\eta + \frac{r_o\mu}{\delta\rho}\int_o^1 \frac{\partial^2 v_s}{\partial\eta^2}\, d\eta \qquad (19)$$

Assuming a profile relation for the velocity in the boundary layer:

$$v_s = v_{s_\delta}\lambda(\eta) \quad \text{where} \quad v_{s_\delta} = f(s) \qquad (19a)$$

$$\int_o^1 v_s^2\, d\eta \longrightarrow \int_o^1 v_{s_\delta}^2\ \lambda(\eta)^2 d\eta \longrightarrow K_1 v_{s_\delta}^2 \qquad (19b)$$

$$\int_o^1 v_s\, d\eta \longrightarrow \int_o^1 v_{s_\delta}\lambda(\eta)\, d\eta \longrightarrow K_2 v_{s_\delta} \qquad (19c)$$

$$\int_o^1 d\eta \longrightarrow 1 \qquad (19d)$$

$$\int_o^1 \frac{\partial}{\partial\eta}\left(\mu\frac{\partial v_s}{\partial\eta}\right)d\eta \longrightarrow -\mu\left(\frac{\partial v_s}{\partial\eta}\right)_{\eta=o} \qquad (19e)$$

Also consider the Bernoulli equation: $\rho\frac{v_{s_\delta}^2}{2} + P_\delta = P_o \qquad (19f)$

Upon differentiation of (19f) with respect to s it immediately follows

$$-\frac{1}{\varrho}\frac{dp}{ds} = \frac{d}{ds}\frac{v_{s_\delta}^2}{2} \tag{19g}$$

Inserting relations (19a) through (19g) into equation (19):

$$\frac{d}{ds}\left(r_o \delta v_{s_\delta}^2 K_1\right) - v_{s_\delta}\frac{d}{ds}\left(r_o \delta v_{s_\delta} K_2\right) = \delta\, r_o \frac{d}{ds}\left(\frac{v_{s_\delta}^2}{2}\right) \tag{20}$$

$$- r_o \frac{\mu}{\varrho}\left(\frac{\partial v_s}{\partial \eta}\right)_{\eta = o}$$

Carrying out the indicated differentiation the L.H.S. of equation (20) becomes:

$$r_o v_{s_\delta}^2 (K_1 - K_2)\frac{d\delta}{ds} + \delta\left[\frac{d}{ds}\left(r_o v_{s_\delta}^2 K_1\right) - v_{s_\delta}\frac{d}{ds}\left(r_o v_{s_\delta} K_2\right)\right] \tag{20a}$$

the term $\frac{d}{ds}\left(r_o v_{s_\delta}^2 K_1\right)$ may be written

$$K_1 v_{s_\delta}\frac{d}{ds}\left(r_o v_{s_\delta}\right) + K_1 r_o \frac{d\left(\frac{v_{s_\delta}^2}{2}\right)}{ds} \tag{20b}$$

then equation (20) becomes

$$\left[(K_1 - K_2) r_o v_{s_\delta}^2\right]\frac{d\delta}{ds} + \delta\left[(K_1 - K_2) v_{s_\delta} r_o \frac{d(r_o v_{s_\delta})}{ds} + K_1 r_o \frac{d\left(\frac{v_{s_\delta}^2}{2}\right)}{ds}\right]$$

$$= \delta\, r_o \frac{d}{ds}\left(\frac{v_{s_\delta}^2}{2}\right) - \frac{\mu}{\varrho}\frac{r_o}{\delta}\left(\frac{\partial v_s}{\partial \eta}\right)_{\eta = o} \tag{20c}$$

Dividing by $(K_1 - K_2) r_o v_{s_\delta}^2$ and multiplying by δ :

$$\frac{d\delta^2}{ds} + \delta^2\left[\frac{2}{r_o v_{s_\delta}}\frac{d(r_o v_{s_\delta})}{ds} + \left(\frac{K_1 - 1}{K_1 - K_2}\right)\frac{1}{\frac{v_{s_\delta}^2}{2}}\frac{d\left(\frac{v_{s_\delta}^2}{2}\right)}{ds}\right] = -\frac{2\mu}{\varrho (K_1 - K_2) v_{s_\delta}}\left(\frac{\partial \lambda(\eta)}{\partial \eta}\right)_{\eta = o} \tag{20d}$$

Note that $$\frac{2}{r_o v_{s_\delta}} \frac{d(r_o v_{s_\delta})}{ds} = \frac{d \log(r_o v_{s_\delta})^2}{d s} \tag{20e}$$

and $$\frac{K_1 - 1}{K_1 - K_2} \frac{1}{\frac{v_{s_\delta}^2}{2}} \frac{d(\frac{v_{s_\delta}^2}{2})}{ds} = \frac{d}{ds}(\log (\frac{v_{s_\delta}^2}{2})^{\frac{K_1 - 1}{K_1 - K_2}} \tag{20f}$$

With relations (20e), (20f) the equation (20d) becomes

$$\frac{d\delta^2}{ds} + \delta^2 \frac{d}{ds}\left[\log(r_o v_{s_\delta})^2 + \log(\frac{v_{s_\delta}}{2})^{2\frac{K_1 - 1}{K_1 - K_2}}\right] = - \frac{2\nu}{(K_1 - K_2) v_{s_\delta}} (\frac{\partial \lambda(\eta)}{\partial \eta})_{\eta = o} \tag{21}$$

This differential equation can be immediately integrated to the following form:

$$\delta^2 = \frac{-2\nu}{(K_1 - K_2)} (\frac{\partial \lambda(\eta)}{\partial \eta})_{\eta = o} \frac{\int_o^s \frac{(r_o v_{s_\delta})^2 (\frac{v_{s_\delta}}{2})^{2\frac{K_1 - 1}{K_1 - K_2}}}{v_{s_\delta}} ds}{(r_o v_{s_\delta})^2 (\frac{v_{s_\delta}}{2})^{2\frac{K_1 - 1}{K_1 - K_2}}} \tag{22}$$

where $$\left.\begin{aligned} K_1 &= \int_o^1 \lambda(\eta)^2 \, d\eta \\ K_2 &= \int_o^1 \lambda(\eta) \, d\eta \end{aligned}\right\} \; ; \quad \lambda(\eta) = \frac{v_s}{v_{s_\delta}} \tag{22a}$$

With the assumption of a profile relation as equation (12), equation (22) reduces immediately to

$$\delta^2 = \frac{56.1 \, \nu}{(r_o v_{s_\delta})^2 (\frac{v_{s_\delta}}{2})^{2\,3.34}} \int_o^s \left[\frac{(r_o v_{s_\delta})^2 (\frac{v_{s_\delta}^2}{2})^{3.34}}{v_{s_\delta}}\right] ds \tag{23}$$

Equation (23) bears a marked resemblance to the equation developed for a case similar to Case III in reference 6. It can readily be reduced to a variation of δ with s by means of graphical integration. E.

Case IV Incompressible Flow with No Pressure Gradient

Starting with equation (20) under Case III and noting that $\frac{dp}{ds} = 0$, and v_{s_δ} is independent of s, the basic equation for Case IV is

$$v_{s_\delta}{}^2 \left[\frac{d}{ds}(r_o \delta K_1) - \frac{d}{ds}(r_o \delta K_2) \right] = - \frac{r_o \nu}{\delta} \left(\frac{\partial v_s}{\partial \eta} \right)_{\eta = o} \qquad (24)$$

this equation reduces immediately to

$$\frac{d\delta^2}{ds} + \delta^2 \frac{d \log r_o^2}{ds} = - \frac{2\nu \left(\frac{\partial \lambda(\eta)}{\partial \eta} \right)_{\eta = o}}{v_{s_\delta} (K_1 - K_2)} \qquad (24a)$$

the solution to this equation is

$$\delta^2 = \frac{- 2\nu \left(\frac{\partial \lambda(\eta)}{\partial \eta} \right)_{\eta = o}}{v_{s_\delta} (K_1 - K_2)} \frac{\int_o^s r_o{}^2 ds}{r_o{}^2} \qquad (25)$$

Assuming the velocity profile as in equation (12), equation (25) reduces to

$$\delta^2 = \frac{56.1 \nu}{v_{s_\delta}} \frac{\int_o^s r_o{}^2 ds}{r_o{}^2} \qquad (26)$$

It is interesting to note the similarity that equation (26) bears to the flat plate solution as given in reference 10, Assuming that the axial symmetric body is a cone, the

$$\int_o^s \frac{r_o{}^2 \, ds}{r_o{}^2} = \frac{s}{3}$$

then equation (26) reduces to

$$\delta^2 = \frac{18.7 \nu s}{v_{s_\delta}} \tag{26a}$$

or $$\delta = 4.33 \sqrt{\frac{\nu s}{v_{s_\delta}}} \tag{26b}$$

From Durand Volume III, Page 90, the flat plate solution is given as

$$\delta = 5.20 \sqrt{\frac{\nu s}{u_\infty}} \tag{26c}$$

It should be pointed out however that (26c) is based on a parabolic distribution of velocity in the boundary layer whereas the constant of equation (26b) is based on a cubic variation of velocity. Using the identical velocity profile for the cone and flat plate yields the well known $\sqrt{3}$ difference between boundary layer thickness for these two bodies.

SECTION II

DEVELOPMENT OF EXPRESSIONS FOR SKIN FRICTION DRAG, DRAG COEFFICIENT

Skin Friction Drag:

The skin friction drag for the axial symmetric body is the integral of the axial component of skin friction force over the entire body. The skin friction force per unit area is defined as

$$\tau = \mu_o \left(\frac{\partial v_s}{\partial n}\right)_{n=o} \tag{27}$$

From equation (12) $v_s = v_{s_\delta} (3\eta - 3\eta^2 + \eta^3)$ where $\eta = \frac{n}{\delta}$

then $$\frac{\partial v_s}{\partial n} = \frac{\partial v_s}{\partial \eta} \frac{\partial \eta}{\partial n} = v_{s_\delta} (3 - 6\eta + 3\eta^2) \frac{1}{\delta}$$

and at $n = 0$ $$\frac{\partial v_s}{\partial n} = \frac{3 v_{s_\delta}}{\delta}$$

Equation (27) becomes $$\tau = \frac{3 \mu_o v_{s_\delta}}{\delta} \tag{27a}$$

The area under consideration as shown by the figure:

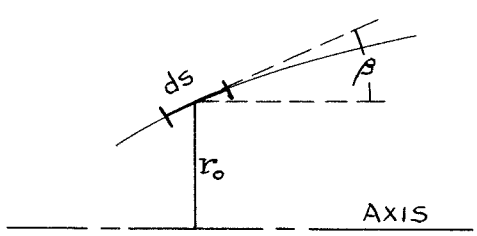

$$dA = 2\pi r_o \cos\beta \, ds \tag{27b}$$

The total skin friction drag acting on the body is

$$D = \int_o^s \tau \, dA = 6\pi\mu_o \int_o^s \frac{v_{s\delta} \, r_o \cos\beta}{\delta} \, ds \tag{28}$$

Skin Friction Drag Coefficient

The skin friction drag coefficient is defined as

$$C_D = \frac{\text{Drag}}{q \, A} \tag{29}$$

where $q = \frac{\gamma}{2} P_\infty M^2$

or $q = \frac{1}{2} \rho v_\infty^2$

SELECTION OF BOUNDARY LAYER VELOCITY PROFILE AND THE EFFECT OF VARIOUS PROFILES ON DRAG COEFFICIENT

A. General Considerations

In the Polhausen method for the solution of the approximate boundary layer equations for boundary layer thickness and drag, one makes use of an assumed velocity profile relation of the form

$$\frac{v_s}{v_{s_\delta}} = a + b\left(\frac{n}{\delta}\right) + c\left(\frac{n}{\delta}\right)^2 + \cdots$$

where a, b, c, etc. are constants determined by the boundary conditions at the surface ($n = 0$), and at the outer edge of the boundary layer ($n = \delta$). Fair agreement between theory and experimental values can be had by selecting a linear or a parabolic profile relation, but the assumption of a cubic or quadratic relation yields better agreement. Some of the boundary conditions that must be applied are valid for all steady state laminar flow such as

$$\text{at } \eta = 1 \qquad v_s = v_{s_\delta}$$

$$\frac{\partial v_s}{\partial \eta} = 0$$

$$\text{at } \eta = 0 \qquad v_s = v_n = 0$$

$$\text{where} \qquad \eta = \frac{n}{\delta}$$

These three conditions are sufficient to determine either the linear or the parabolic relation. Some care must be exercised in the selection of further boundary conditions since it will later be shown that the profile selected has an appreciable effect on the value of skin friction

drag.

To gain an insight of the further boundary conditions which should be imposed it is quite useful to study the boundary layer momentum equation:

$$\rho v_n \frac{\partial v_s}{\partial n} + \rho v_s \frac{\partial v_s}{\partial s} = -\frac{dp}{ds} + \mu \frac{\partial^2 v_s}{\partial n^2} + \frac{\partial v_s}{\partial n} \frac{\partial \mu}{\partial n}$$

Now considering conditions at the surface, it can be said $v_n = v_s = 0$ and $\frac{\partial \mu}{\partial n} = 0$ this latter can be seen by differentiating the energy equation, $T_o = T + \frac{1}{2C_p} v_s^2$

$$0 = \frac{\partial T}{\partial n} + \frac{1}{C_p} v_s \frac{\partial v_s}{\partial n}$$

$$\text{or} \qquad \frac{\partial T}{\partial n} = 0 \qquad \therefore \quad \frac{\partial \mu}{\partial n} = 0$$

With these conditions the momentum equation reduces to

$$\left(\frac{\partial^2 v_s}{\partial n^2}\right)_{n=o} = \frac{1}{\mu} \frac{dp}{ds}$$

This equation indicates that for a flat plate (zero pressure gradient), $\left(\frac{\partial^2 v_s}{\partial n^2}\right)_{n=o} = o$ should be a condition imposed on the profile relation. However, if a favorable pressure gradient is known to exist then $\frac{\partial^2 v_s}{\partial n^2}$ should be negative and of a certain order of magnitude. Since inserting $\frac{1}{\mu} \frac{dp}{ds}$ at each station along s would yield a varying profile relation

along s, it is deemed sufficient in this case to select a boundary layer profile relation which would yield an approximately correct value for $\partial^2 v_s / \partial n^2$ at $n = 0$, and to keep this profile constant along s. The condition which is selected for the boundary layer profile relation in this thesis is $\frac{\partial^2 v_s}{\partial n^2} = 0$ at $\eta = 1$. It is shown to result in the correct sign and approximate order of magnitude for $\frac{\partial^2 v_s}{\partial n^2}$ at $\eta = 0$, a posteriori.

The following table serves to show the boundary conditions and the profile relations resulting by insertion of the conditions into the general form

$$v_s = v_{s_\delta} (a + b\eta + c\eta^2 + \cdots)$$

TABLE II

BOUNDARY LAYER VELOCITY PROFILES

	Type of Equation	$\frac{dp}{ds}$	η	v_s	$\frac{\partial v_s}{\partial \eta}$	$\frac{\partial^2 v_s}{\partial \eta^2}$	$\frac{\partial^3 v_s}{\partial \eta^3}$	Profile Relation
#1	Linear		0 1	0 v_{s_δ}				$v_s = v_{s_\delta} \eta$
#2	Quadratic		0 1	0 v_{s_δ}	0			$v_s = v_{s_\delta} (2\eta - \eta^2)$
#3	Cubic	0	0 1	0 v_{s_δ}	0	0		$v_s = v_{s_\delta} (\frac{3\eta}{2} - \frac{\eta^3}{2})$
#4	Quartic	0	0 1	0 v_{s_δ}	0	0 0		$v_s = v_{s_\delta} (2\eta - 2\eta^3 + \eta^4)$
#5	Cubic	-	0 1	0 v_{s_δ}	0	0		$v_s = v_{s_\delta} (3\eta - 3\eta^2 + \eta^3)$
#6	Quartic	-	0 1	0 v_{s_δ}	0	0	0	$v_s = v_{s_\delta} (4\eta - 6\eta^2 + 4\eta^3 - \eta^4)$

A plot of $\lambda(\eta)$ vs η where $\lambda(\eta) = \frac{v_s}{v_{s_\delta}}$ is is shown in Figure 2.

The relation selected for use throughout this analysis is $v_s = v_{s_\delta}(3\eta - 3\eta^2 + \eta^3)$. It was selected for its relative simplicity and for its reasonably accurate representation of conditions at the surface for the case of a favorable pressure gradient. This will be shown below. Equations are also presented for comparing drag values obtained by the use of this relation with those obtained by the other relations.

B. A Posteriori Check of Validity of Profile Relation Selected

It was shown above that for the case with a pressure gradient

$$\left(\frac{\partial^2 v_s}{\partial n^2}\right)_{n=o} = \frac{1}{\mu}\frac{dp}{ds}$$

Selecting values for the case $M = 1.87$ at a point where $v_{s_\delta} = v_\infty$

$$\frac{1}{\mu}\frac{dp}{ds} = -\frac{2200(.2)}{3.76 \times 10^{-7}} = -1.17 \times 10^9 \quad \text{ft.}^{-1}\,\text{sec.}^{-1}$$

For the profile selected $v_s = v_{s_\delta}(3\eta - 3\eta^2 + \eta^3)$

$$\left(\frac{\partial^2 v_s}{\partial \eta^2}\right)_{\eta=o} = -6\, v_{s_\delta}$$

or

$$\left(\frac{\partial^2 v_s}{\partial n^2 n}\right)_{n=o} = \frac{-6\, v_{s_\delta}}{\delta^2}$$

$$= -\frac{6\,(1627)}{3.32 \times 10^{-6}} = -3 \times 10^9 \quad \text{ft.}^{-1}\,\text{sec.}^{-1}$$

It is seen that the profile relation yields the correct sign but a somewhat higher order of magnitude than is demanded by the boundary

FIG. 2 BOUNDARY LAYER PROFILES

#1. $\lambda(\eta) = \eta$

#2. $\lambda(\eta) = 2\eta - \eta^2$

#3. $\lambda(\eta) = 1.5\eta - 0.5\eta^3$

#4. $\lambda(\eta) = 2\eta - 2\eta^3 + \eta^4$

#5. $\lambda(\eta) = 3\eta - 3\eta^2 + \eta^3$

#6. $\lambda(\eta) = 4\eta - 6\eta^2 + 4\eta^3 - \eta^4$

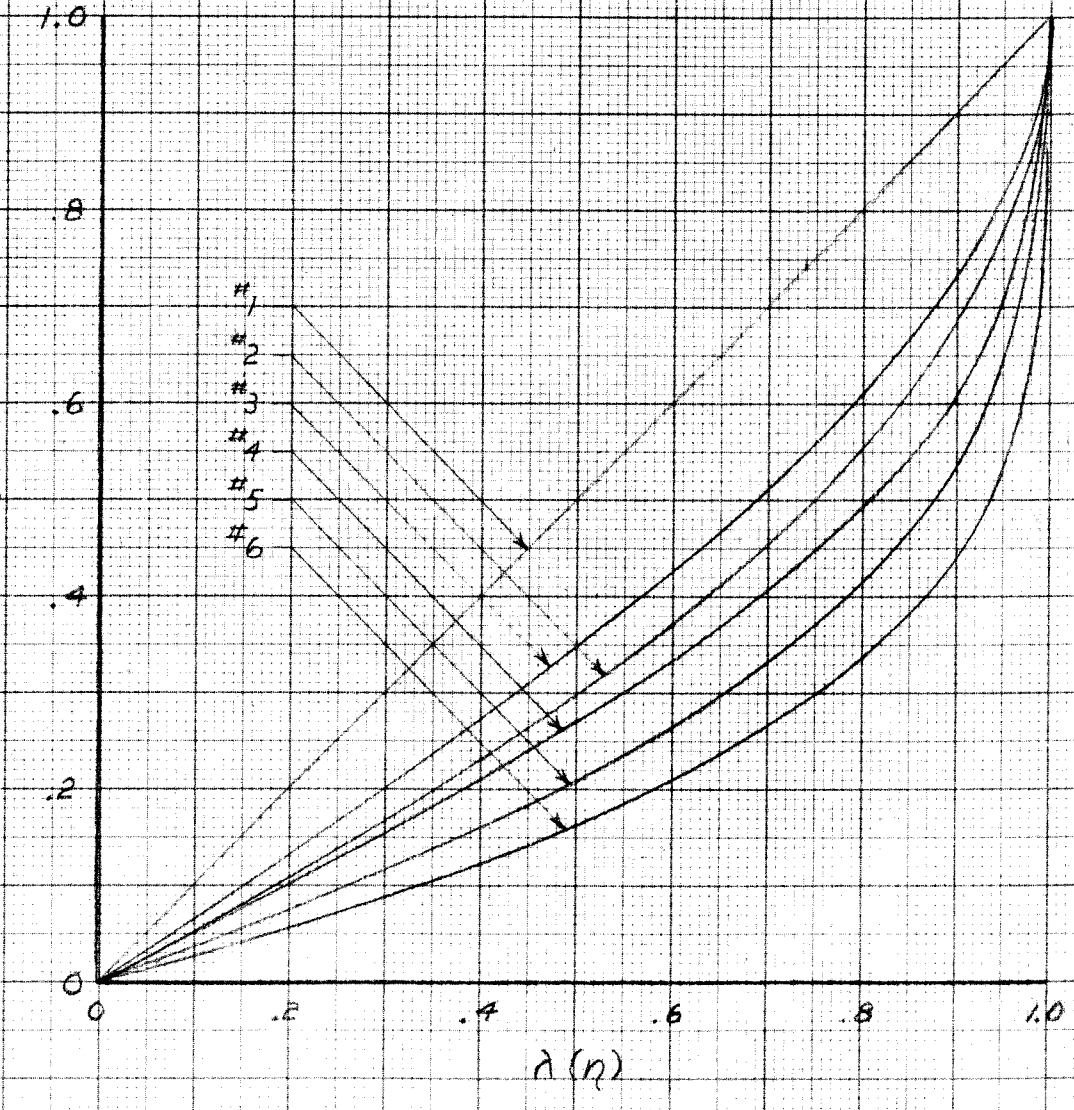

layer momentum equation at the surface. Consequently the proper profile relation lies between this relation 5 and relation 4 which has

$$\left(\frac{\partial^2 v_s}{\partial \eta^2}\right)_{\eta = o} = 0 .$$

C. Effect of Profile Relation on Drag Coefficient Ratios

Since the profile relation used throughout this investigation is strictly valid only in the case where a favorable pressure gradient exists, it is necessary to obtain formulas for conversion of the drag values obtained to values which would have resulted if more valid profile relations were used. In addition to this comparison of C_D values at the same Reynolds and Mach numbers, it is also of interest to obtain a relation between C_D values obtained using an identical profile relation at different RN and M. To these ends the following equations are developed:

For compressible flow from equations (28) and (29)

$$C_D = \frac{2\pi \mu_o \left(\frac{\partial v_s}{\partial \eta}\right)_{\eta = o} \int_o^s \frac{v_s \; r_o \cos \beta}{\delta} \, ds}{\frac{\gamma}{2} P_\infty M^2 A}$$

but

$$\delta = \sqrt{\frac{- 2\pi \mu_o \left(\frac{\partial v_s}{\partial \eta}\right)_{\eta = o} v_{s_\delta} \int_o^s r_o^2 \, ds}{\frac{\gamma}{\gamma - 1} P_\infty \left(C_1 - v_{s_\delta} \sqrt{\frac{2}{C_p T_o}} \; C_2\right) r_o^2}}$$

Now considering that no pressure gradient exists, i.e., v_{s_δ} , C_1 , C_2 are constant.

$$C_D = \frac{2\pi}{M^2}\sqrt{-\frac{2}{\gamma(\gamma-1)}}\,\frac{\mu_o v_{s_\delta}\left(C_1 - v_{s_\delta}\sqrt{\frac{2}{C_pT_o}}\,C_2\right)\left(\frac{\partial\lambda(\eta)}{\partial\eta}\right)_{\eta=o}}{P_\infty}\int_o^s \frac{r_o^2\cos\beta}{\sqrt{\int_o^s r_o^2 ds}}\,ds \qquad (29a)$$

Comparing C_D values at the same M, and RN but using different profile relations, there is obtained:

$$\left(\frac{C_{D_1}}{C_{D_2}}\right)_{A_C} = \sqrt{\frac{\left[\left(C_1 - v_{s_\delta}\sqrt{\frac{2}{C_pT_o}}\,C_2\right)\left(\frac{\partial\lambda(\eta)}{\partial\eta}\right)_{\eta=o}\right]_1}{\left[\left(C_1 - v_{s_\delta}\sqrt{\frac{2}{C_pT_o}}\,C_2\right)\left(\frac{\partial\lambda(\eta)}{\partial\eta}\right)_{\eta=o}\right]_2}} \qquad (29b)$$

For the incompressible case a similar relation may be developed:

$$\left(\frac{C_{D_1}}{C_{D_2}}\right)_{A_i} = \sqrt{\frac{\left[(K_1 - K_2)\left(\frac{\partial\lambda(\eta)}{\partial\eta}\right)_{\eta=o}\right]_1}{\left[(K_1 - K_2)\left(\frac{\partial\lambda(\eta)}{\partial\eta}\right)_{\eta=o}\right]_2}} \qquad (29c)$$

wherein C_1, C_2, K_1, K_2 are given in equations (13b), (13c), (19b), (19c) respectively.

Tables III and IV show the effect of profile relation on C_D values for the compressible and incompressible cases respectively.

TABLE III

EFFECT OF PROFILE ON C_D, COMPRESSIBLE

Profile	$\left(\frac{\partial \lambda(\eta)}{\partial \eta}\right)_{\eta=0}$	$C_1 - v_{s_\delta}\sqrt{\frac{2}{C_p T_o}}\, C_2$		C_D	
		M = 1.56	M = 1.87	M = 1.56	M = 1.87
#1 Linear	1	-.1233	-.1578	.000836	.000870
#2 Parabolic	2	-.09891	-.1311	.001053	.001124
#3 Cubic	3/2	-.10315	-.13826	.000936	.000997
#4 Quartic	2	-.0905	-.1208	.001013	.001076
#5 Cubic	3	-.0853	-.0965	.001205	.001179
#6 Quartic	4	-.07891	-.07740	.001338	.001220

TABLE IV

EFFECT OF PROFILE ON C_D, INCOMPRESSIBLE

Profile	$K_1 - K_2$ v_∞, R_e ⟶ M = 1.87	C_D v_∞, R_e ⟶ M = 1.87
#1 Linear	-0.1666	0.000925
#2 Parabolic	-0.1333	0.001150
#3 Cubic	-0.1393	0.001020
#4 Quartic	-0.1175	0.001103
#5 Cubic	-0.1070	0.001261
#6 Quartic	-0.0888	0.001330

Now considering the effect of M and RN on C_D ratio using the identical profile relation for each case: The ratio of C_D's may be written from equation (29a) as

$$\frac{C_{D_1}}{C_{D_2}} = \frac{M_{\infty 2}^2}{M_{\infty 1}^2} \sqrt{\frac{\mu_{o1}\, v_{s\delta 1}\, P_{\infty 2}\, (C_1 - v_{s\delta}\sqrt{\frac{2}{C_p T_o}}\, C_2)_1}{\mu_{o2}\, v_{s\delta 2}\, P_{\infty 1}\, (C_1 - v_{s\delta}\sqrt{\frac{2}{C_p T_o}}\, C_2)_2}}$$

For the two cases dealt with in this investigation:

(cubic profile relation 5)

$M_1 = 1.87 \quad v_{s\delta 1} = 1610 \quad P_{\infty 1} = 350 \quad (C_1 - v_{s\delta}\sqrt{\frac{2}{C_p T_o}}\, C_2)_1 = -.0965$

$M_2 = 1.56 \quad v_{s\delta 2} = 1440 \quad P_{\infty 2} = 547 \quad (C_1 - v_{s\delta}\sqrt{\frac{2}{C_p T_o}}\, C_2)_2 = -.0853$

and $\frac{C_{D_1}}{C_{D_2}} = .978$

This ratio may be compared to that predicted by Emmons and Brainerd (reference 1) for a flat plate in compressible flow using a Prandtl number $\sigma = 1$. For the same RN and M as used here values of C_D are

$M = 1.87 \quad RN = 1.743 \times 10^6 \quad C_D = .000962$
$M = 1.56 \quad RN = 1.932 \times 10^6 \quad C_D = .000925$

$$\frac{C_{D_1}}{C_{D_2}} = 1.04$$

The following table shows the effect of profile relation on C_D ratio as would be predicted between the M and RN used.

TABLE V

C_D RATIO FOR DIFFERENT M AND RN AS EFFECTED BY PROFILE

Profile Relation	C_{D_1}/C_{D_2}
#1 Linear	1.042
#2 Parabolic	1.060
#3 Cubic	1.068
#4 Quartic	1.064
#5 Cubic	.978
#6 Quartic	.946
Emmons and Brainerd	1.04
Blasius	1.05

SECTION IV

PRESENTATION OF EXPERIMENTAL DATA

For purposes of numerical computation in the application of the equations developed under Section I, II, the axial symmetric body chosen was a $\frac{3}{140}$ size model of the German V-2 rocket which was tested in a Peenemünde supersonic wind tunnel and for which pressure distribution data and physical characteristics were reported in references 11, 12. It should be noted that only the nose of the model size V-2 rocket, over which a favorable pressure gradient exists, is treated in this analysis.

Pressure Distribution Data

References 11, 12 present data for two Mach numbers and two Reynolds numbers as shown in Table VI below:

TABLE VI

PRESSURE DISTRIBUTION FOR MODEL V-2 NOSE

AT ZERO ANGLE OF ATTACK

M	1.87	1.56
R_e*	4.14×10^6	4.59×10^6
R_e**	1.743×10^6	1.932×10^6
x(ft.)	P/P_o	P/P_o
0	0.248	0.360
0.0563	0.225	0.332
0.1125	0.203	0.308
0.1689	0.184	0.285
0.2253	0.170	0.265
0.271	0.156	0.245
0.338	0.143	0.227
0.379	0.132	0.215
Undisturbed stream	0.159	0.249

For purposes of simplification the arc length along the nose is assumed to be identical to the axial distance at any point (actually at $x = 0.415$, $s = 0.424$), and analytical expressions are developed for the dependence of P/P_o on s.

For $M = 1.87$, $P/P_o = 0.05575 + 0.1923\ e^{-2.345s}$ (31)

and for $M = 1.56$ $P/P_o = 0.1018 + 0.2582\ e^{-2.09s}$ (31a)

These expressions and the corresponding experimental data are shown plotted in Figure 3.

Physical Characteristics of the Model V-2 Nose

The model V-2 nose is an ogival form whose radius of curvature is 11.8 caliber, whose length is 3.4 caliber, and whose diameter is

---

R_e* based on model size full missile axial length (.985 ft.)
R_e** based on model size nose axial length (.415 ft.)
x is axial distance from upstream end of nose.

0.122 ft. An analytic expression for $r_o(s)$ is developed under the computation section and is given as

$$r_o = 1.44 \sin(39.8s + 73.13)^o - 1.379 \qquad (32)$$

Other pertinent physical characteristics useful for computation purposes are:

Wetted Area = 0.1089 ft^2

Angle of tangent β, see (27b) = $(16.9 - 39.8s)^o$

Other useful values such as r_o, $r_o \cos\beta$ and $\frac{\int_o^s r_o^2 \, ds}{r_o^2}$ are given in table XVIII and XIV under Appendix I.

SECTION V

DEVELOPMENT OF DATA FOR USE IN EVALUATING BOUNDARY LAYER THICKNESS AND SKIN FRICTION DRAG

A. Compressible Flow

The solution of equations (16) and (18) require a knowledge μ, v_{s_δ}, T_o, pressure distribution, etc. It is therefore necessary to develop the data given under Section III in a form suitable for use in the application of the equations.

Consider first the data for $M = 1.87$:

Assume an absolute temperature stagnation value = 528°R (68°F)

Now using the relation $\frac{T_o}{T_\infty} = 1 + \frac{\gamma - 1}{2} M_\infty^2$, T_∞ can be found to be 311°R. These two values T_∞, T_o in combination with

$$C_p \ (= 5997 \text{ ft}^2 \text{ sec}^{-2} \text{ of}^{-1})$$

and equation (14) yield a free stream velocity $v_\infty = 1610$ ft sec^{-1}. Also from reference 13 the stagnation viscosity coefficient,

$$\mu_o = 3.76 \times 10^{-7} \text{ slugs ft}^{-1} \text{ sec}^{-1}.$$

Assuming an 0.76 variation of viscosity coefficient ratio with temperature ratio, μ_∞ (the free stream viscosity coefficient) becomes 2.52×10^{-7} slugs ft^{-1} sec^{-1}. These free stream values when used in conjunction with the RN of test yield a free stream density, $\rho_\infty = 0.00066$ slugs ft^{-3}. Now from the two expressions for dynamic pressure, $q_\infty = \frac{1}{2} \rho_\infty v^2 = \frac{\gamma}{2} M_\infty^2$, it is found that free stream pressure, $p_\infty = 350$ lb ft^{-2}. Stagnation pressure, $P_o = \frac{P_\infty}{.159}$ = 2200 lb - ft^{-2} and through the equation of state it is found that

$\rho_o = 0.00243$ slug ft^{-3}.

The data for $M = 1.56$ may be treated in a similar fashion. The two sets of data are collected in Table VII.

TABLE VII

DATA FOR MATCHING M AND RN

(assuming $T_o = 528^oR$)

			Units
M	1.87	1.56	
RN	4.14×10^6	4.59×10^6	
T_o	528	528	^oR
T_∞	311	354	^oR
P_o	2200	2200	lb - ft^{-2}
P_∞	350	547	lb - ft^{-2}
μ_o	3.76×10^{-7}	3.76×10^{-7}	slugs - ft^{-1} - sec^{-1}
μ_∞	2.52×10^{-7}	2.78×10^{-7}	slugs - ft^{-1} - sec^{-1}
ρ_o	0.00243	0.00243	slugs - ft^{-3}
ρ_∞	0.00066	0.000900	slugs - ft^{-3}
v_∞	1610	1440	ft - sec^{-1}
q_∞	857	933	lb - ft^{-2}

B. Incompressible Flow

For the treatment of the incompressible flow equations (23), (26) it is desirable to match RN and pressure distribution as applied to the equations for compressible flow. This will be done for the set of data obtained at an $M = 1.87$. Start with Bernoulli's equation for incompressible flow.

$$\frac{\rho}{2} v_{s_\delta}^2 + P_\delta = P_o \tag{33}$$

From this equation

$$v_{s_\delta} = \sqrt{2 \frac{P_o}{\rho} \left(1 - \frac{P_\infty}{P_o} \right)} \tag{33a}$$

The pressure distribution $\frac{p}{p_o}$ is taken from the data given for $M = 1.87$. Hence $\frac{p_o}{\rho}$ must be chosen so that the given RN are matched for both the compressible and the incompressible cases.

Now consider that the free stream velocity $v_\infty = \sqrt{2 \frac{P_o}{\rho} (1 - \frac{P_\infty}{P_o})}$ (33b)

where $\frac{P_\infty}{P_o}$ is taken from the data. This equation may be solved for

$$\frac{P_o}{\rho} = \frac{v_\infty^2}{2(1 - \frac{P_\infty}{P_o})} \tag{33c}$$

Knowing that $R_e = \frac{\rho v_\infty L}{\mu}$

$$v_\infty^2 = (\frac{\mu}{\rho L})^2 R_e^2 \tag{33d}$$

where R_e may be taken from the data. Inserting equation (33d) into (33c) it is found that

$$\frac{P_o}{\rho} = \frac{(\frac{\mu}{\rho L})^2 R_e^2}{2 (1 - \frac{P_\infty}{P_o})} \tag{33e}$$

Now calling attention to the viscous term in equation (21) it is seen that the viscous term $\backsim \frac{\mu}{\rho v_{s_\delta}}$ (33f). However, from equation (33e)

$$\frac{\mu}{\rho} = \frac{L}{R_e} \sqrt{2 \frac{P_o}{\rho} (1 - \frac{P_\infty}{P_o})} \tag{33g}$$

and from equation (33a) it is seen that (33f) reduces to

$$\text{viscous term} \backsim \frac{L}{R_e} \sqrt{\frac{1 - \frac{P_\infty}{P_o}}{1 - \frac{P}{P_o}}} \tag{33h}$$

Hence the viscous term appears to be independent of the choice of $\frac{P_o}{\rho}$ if the Reynolds number and the pressure distribution are matched. Consequently let μ_o and $\frac{P_\infty}{P_o}$ be the same as they were for $M = 1.87$.

$$\mu = 3.76 \times 10^{-7} \text{ slugs ft}^{-1} \text{ sec}^{-1}$$
$$P_o = 2200 \text{ lb - ft}^{-2}$$
$$P_\infty = 350 \text{ lb - ft}^{-2}$$
$$R_e = 4.14 \times 10^{-6}$$
$$L = 0.985 \text{ ft} \quad \text{(complete missile)}$$

Using these values in equation (33e)

$$\rho = 0.000677 \text{ slugs ft}^{-3}$$

and from equation (33a)

$$v_{s_\delta} = 2.55 \times 10^3 \sqrt{1 - \frac{P}{P_o}} \qquad (33i)$$

SECTION VI

DISCUSSION OF RESULTS

Boundary Layer Thickness

Boundary layer thicknesses evaluated through the use of the cubic profile relation 5 are shown in Table VIII and Figures 4 and 5.

Figure 4 shows the variation in boundary layer thickness along the surface of the ogive for M = 1.87 for the four cases considered. This figure clearly shows the effects of a favorable pressure gradient and compressibility on the thickness. In general a favorable pressure gradient retards the growth of the boundary layer. On the other hand the introduction of compressibility causes the boundary layer to thicken (Figure 2, reference 14). Figure 5, which is for M = 1.56, again illustrates the effect of a favorable pressure gradient.

A comparison between the thicknesses for the two M's shows a considerably larger value of δ for M = 1.87 than for M = 1.56. Figure 2 of reference 14 indicates a decrease in boundary layer thickness with an increase in M.

From equation (18) it can be shown that for a given profile relation, and zero pressure gradient,

$$\frac{\delta_1}{\delta_2} = \sqrt{\frac{v_{s_{\delta 1}}}{v_{s_{\delta 2}}} \frac{P_2}{P_1} \frac{\left(C_1 - v_{s_\delta} \sqrt{\frac{2}{C_p T_o}}\ C_2\right)_2}{\left(C_1 - v_{s_\delta} \sqrt{\frac{2}{C_p T_o}}\ C_2\right)_1}}$$

Insertion of values for $M_1 = 1.87$, and $M_2 = 1.56$ results in ratios of 1.14, 1.06, 1.25 for profile relations 3, 4, and 5 respectively. Consequently there is an indication that even using a more valid

profile relation (3, 4) the boundary layer is thicker for the higher M. Of course the effect of RN is present but it cannot be discerned very clearly in the form of the above relation of δ ratio. The lower Reynolds number for M = 1.87 must be held accountable for some of the increase in boundary layer thickness.

Skin Friction

In order to present a clear description of compressibility, velocity profile, and pressure gradient effects using the C_D values appearing in Table IX, it is considered instructive to break down the overall comparison into groups and to discuss the effects apparent in each group.

1. Compressibility Effects

(a) Flat Plate Values

From the following table:

M	RN	C_{D_i} (incomp.)	C_{D_c} (comp.)	$\frac{C_{D_c} - C_{D_i}}{C_{D_i}}$ (%)
1.56	1.932×10^6	0.000956	0.000925	-3.24
1.87	1.743×10^6	0.001006	0.000964	-4.18

which are the Blasius and Emmons and Brainerd values, it is apparent that compressibility decreases the C_D for each M and to a greater degree for the higher M. It can also be seen that Reynolds number effects are preserved when going from the incompressible case to the compressible case.

(b) V-2 Ogive with No Pressure Gradient

The values selected in the table below were obtained using the velocity profile 4 for reasons which will be discussed later.

TABLE VIII SUMMARY OF RESULTS ON BOUNDARY LAYER THICKNESS

	COMPRESSIBLE							INCOMPRESSIBLE				
PRESSURE GRAD.	WITH		WITHOUT					WITH	WITHOUT		FLAT PLATE	
M	1.87	1.56	1.87	1.87	1.56	1.56		1.87	1.87	1.87	1.87	1.87
$Re_{(10^6)}$ FREE STREAM	1.743	1.932		1.743		1.932		1.743		1.743		1.743
NOSE VALUE			2.48		2.04				1.648		1.648	
U_{S_δ} (ft/s) FREE STREAM				1610		1440				2340		2340
NOSE VALUE			1444		1264				2210		2210	
S (FT.)	δ (10^{-3} FT.)											
0.000	0.000	0.000	0.000	0.000	0.000	0.000		0.000	0.000	0.000	0.000	0.000
0.025	0.394	0.342	0.454	0.557	0.400	0.448		0.387	0.377	0.367	0.412	0.397
0.050	0.593	0.512	0.605	0.743	0.532	0.598		0.493	0.503	0.489	0.583	0.561
0.100	0.865	0.723	0.871	1.069	0.766	0.860		0.686	0.725	0.705	0.825	0.795
0.150	1.119	0.910	1.061	1.301	0.935	1.048		0.831	0.881	0.856	1.011	0.972
0.200	1.347	1.096	1.262	1.546	1.110	1.243		0.981	1.043	1.013	1.168	1.124
0.250	1.602	1.280	1.442	1.767	1.269	1.423		1.104	1.191	1.158	1.305	1.257
0.300	1.820	1.470	1.616	1.980	1.421	1.595		1.229	1.339	1.300	1.430	1.381
0.350	2.080	1.649	1.828	2.245	1.609	1.803		1.393	1.518	1.475	1.545	1.485
0.400	2.355	1.850	2.035	2.500	1.791	2.010		1.541	1.693	1.645	1.650	1.590
0.424	2.485	1.945	2.145	2.630	1.889	2.115		1.622	1.781	1.730	1.712	1.650

FIG. 5 BOUNDARY LAYER THICKNESS, δ VS. S

~ M = 1.56 ~

	$dp/ds=0$*	$dp/ds \neq 0$
COMPRESSIBLE	a	b

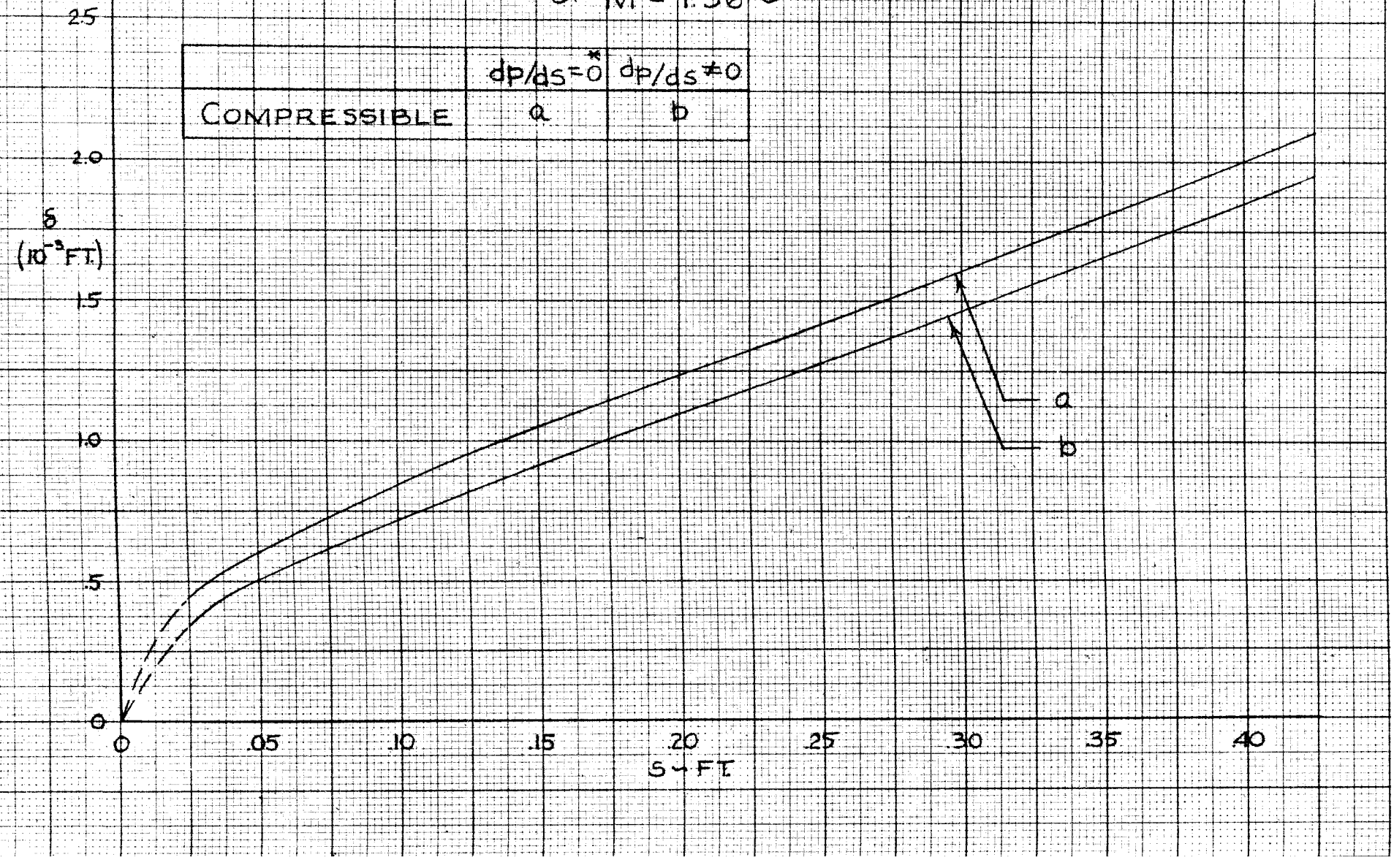

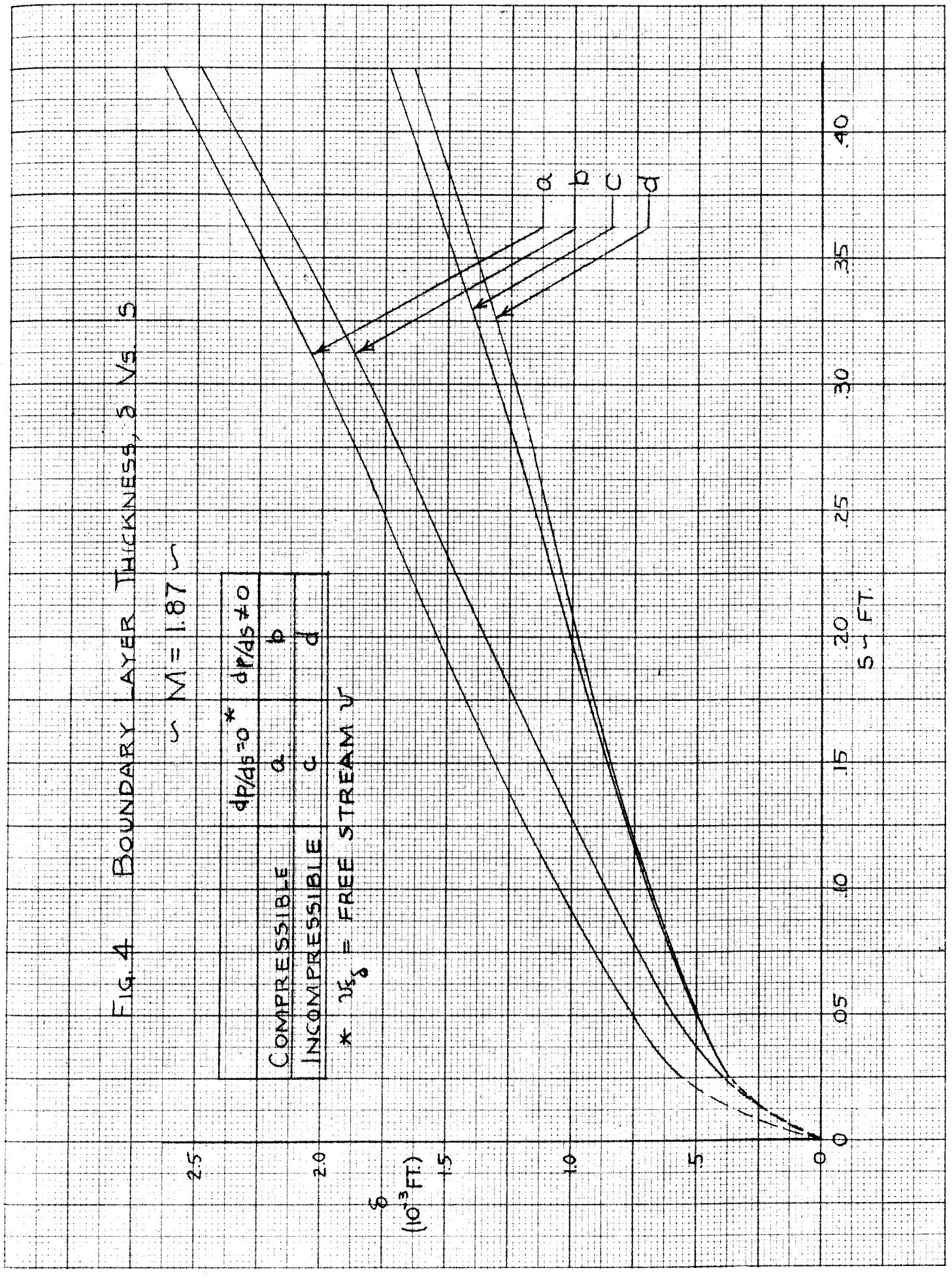
FIG. 4 BOUNDARY LAYER THICKNESS, δ VS. S
M = 1.87
dP/dS = 0 *
dP/dS ≠ 0
COMPRESSIBLE
INCOMPRESSIBLE
a
b
c
d
* u_δ = FREE STREAM u
δ (10⁻³ FT.)
S - FT.
0
.5
1.0
1.5
2.0
2.5
0
.05
.10
.15
.20
.25
.30
.35
.40

M	RN	C_D(incomp.)	C_D(comp.)	$\frac{C_{D_c} - C_{D_i}}{C_{D_i}}$ (%)
1.87	1.743×10^6	0.001103	0.001076	-2.45

It is apparent that a similar reduction in C_D is produced by compressibility as noted under 1(a). Also, it can be noted by comparison with the figures presented in the table under 1(a) that the V-2 ogive with no pressure gradient gives C_D values 10% greater than flat plate predictions for the same conditions.

2. Profile Effects

Referring to Table IX, it is seen that the various assumed velocity profiles have considerable influence on the calculated C_D values. For the three cases considered it is apparent that all profiles with the exception of the linear profile result in values greater than flat plate values.

From the study conducted under Section III it may safely be concluded that only profiles 1, 2, 3, and 4 are valid for the case of no pressure gradient, since the profiles 5 and 6 induce an effective pressure gradient at the surface (i.e., a value of $\frac{\partial^2 v}{\partial n^2}$ is produced at the surface which is in contradiction to the basic momentum equation). The same is also true for profile 2, but it is useful to include the results using this profile. An examination of the value of C_D for any particular case versus the degree of the polynomial selected, 1, 2, 3, and 4, indicates a rapid convergence to the neighborhood of the value given for the profile relation 4. Hence C_D values resulting from the use of this profile relation were used in the comparison for the no pressure gradient case.

Table V shows that profiles 1, 2, 3, and 4, as applied to the compressible no pressure gradient case; are in accord with Emmons and Brainerd flat plate values as to the prediction of combined Mach and Reynolds numbers effects for the two cases studied. However, it should be noted that profiles 5 and 6 predict effects in a direction opposite to Emmons and Brainerd. This opposite effect is then expected to be carried over to the pressure gradient cases wherein these profiles 5 and 6 give a fair representation of the boundary conditions.

3. Pressure Gradient Effects

The following table is used to point out the effects of introducing a pressure gradient over the ogive:

	M	RN	C_{D_o} $(\frac{dp}{ds} = 0)$	C_{D_p} $(\frac{dp}{ds} \neq 0)$	$\frac{C_{D_p} - C_{D_o}}{C_{D_o}}$ (%)
Incompressible	-	1.743×10^6	0.001103	0.001330	11.5
Compressible	1.87	1.743×10^6	0.001076	0.001328	23.4
	1.56	1.932×10^6	0.001013	0.001345	32.8

Comparing the two compressible cases it can be seen that the case for M = 1.56 produces a considerably larger percent change due to pressure gradient. This change could hardly have been expected on the basis of pressure gradient alone. An examination of Figure 3 shows a higher favorable pressure gradient for the M = 1.56 case; however, when referred to dynamic pressure, the pressure gradient for the M = 1.56 case is only 10% greater than for the M = 1.87 case. The reason for the greater percentage increase of ΔC_D may be discerned by a comparison of the C_D values for the profiles 4 and 5 for the case of no pressure gradient. The case, M = 1.56, experiences a 20% increase in C_D whereas

the case, M = 1.87, experiences only a 10% increase when going from the profile 4 for no pressure gradient to the profile 5 for pressure gradient. Consequently pressure gradient effects are twofold. First, they increase the C_D because of the change in the boundary conditions for use in the profile equation, and second, they cause an increase due to retarding the growth of the boundary layer. Again, it should be noted that the results of the effects of Mach number and Reynolds number are opposite to the combined effects predicted by Emmons and Brainerd. In the light of Section III, B, the proper effect lies somewhere between that shown by the use of profile 5 and the Emmons and Brainerd prediction.

An examination of the incompressible and compressible cases for the same Reynolds number shows that the compressible case, in going from no pressure gradient to pressure gradient, experiences a C_D increase twice as great as the incompressible case does. In the light of the above discussion, this result can clearly be understood. First, the introduction of profile 5 increases the C_D 15% for the incompressible case with no pressure gradient against an increase of 10% for the compressible case. Then the much higher dynamic pressure for the incompressible case causes a 55% reduction in its effective pressure gradient.

The fact that the resulting C_D's for the compressible and incompressible cases with pressure gradient are identical is mere coincidence.

It is of interest to note that even basing the compressible C_D with pressure gradient on the nose value of dynamic pressure does not reduce the value of C_D for the ogive to the Blasius C_D value obtained using nose Reynolds number. A discrepancy of approximately 35% exists

for this comparison.

There does not appear to be any consistent basis for comparison between values of C_D obtained by using nose pressure as constant over the ogive with either flat plate values or ogive values obtained by using a pressure gradient.

A comparison of C_D values as calculated for the ogive with pressure gradient with those values predicted for a flat plate by using the Blasius, and the Emmons and Brainerd theories indicates that the current practice of applying incompressible flat plate results to figures of revolution is highly unconservative and is more so if compressible flat plate values are applied. For relatively high Reynolds numbers the skin friction drag is a low percentage of the total drag, hence there is a certain amount of justification in this practice; however, for flights at extremely high altitudes, the Reynolds number is of such an order of magnitude as to cause the skin friction drag to increase greatly. It is true that only the ogival section was considered in this investigation, and it appears that the overall skin friction C_D will be less when considering a longer body over which portions are in a zero or unfavorable pressure gradient. However, it is believed that the entire skin friction C_D will still be considerably above flat plate values (assuming laminar boundary layer to exist over the region).

TABLE IX SUMMARY OF RESULTS ON SKIN FRICTION DRAG

PRESSURE GRAD.	COMPRESSIBLE						INCOMPRESSIBLE							
	WITH		WITHOUT				WITH	WITHOUT		FLAT PLATE			FLAT PLATE (SEE NOTE)	
V_{SS}			NOSE	FREE STREAM	NOSE	FREE STREAM	FREE STREAM	NOSE	FREE STREAM	NOSE	FREE STREAM	FREE STREAM		
M	1.870	1.560	1.870	1.870	1.560	1.560	1.870	1.870	1.870	1.870	1.870	1.560	1.870	1.560
$Re_{(10^6)}$ FREE STREAM	1.743	1.932	1.743	1.743	1.932	1.932	1.743	1.743	1.743		1.743	1.932		
NOSE VALUE			2.480		2.040			1.648		1.648			2.480	2.040
D^* (lb.)	.1239	.1362	.1205	.1100	.1206	.1226	.2940	.2565	.2540					
q FREE STREAM	857	933	857	857	933	933	1850	1850	1850		1850			
NOSE VALUE ($lb\cdot ft^{-2}$)	930	962	930		962			1650		1650			930	962
C_D (q^{**}_{NOSE})	0.001223	0.001302	0.001190		0.001150			0.001297					0.000844	0.000929
C_D ($q_{FREE\ STREAM}$)														
#1. LINEAR PROFILE				.000870		.000836			.000925					
#2. PARABOLIC				.001124		.001053			.001150					
#3. CUBIC				.000997		.000936			.001020					
#4. QUARTIC				.001076		.001013			.001103					
#5. CUBIC	.001328	.001345	.001292	.001179	.001179	.001205	.001330	.001156	.001261					
#6. QUARTIC				.001220		.001338			.001330					
(SEE SECT. III FOR PROFILE DESCRIPTION)														
BLASIUS										.001035	.001006	.000956		
EMMONS & BRAINERD				.000964		.000925								

* DRAG VALUES CORRESPONDING TO CUBIC PROFILE #5

$$q^{**}_{NOSE} = \frac{\gamma}{2} P_{NOSE} M^2_{NOSE}$$

$$q^{**}_{NOSE_{1.87}} = \frac{\gamma}{2} (545)(1.563)^2$$

$$q^{**}_{NOSE_{1.56}} = \frac{\gamma}{2} (742)(1.318)^2$$

NOTE : REYNOLDS NUMBER BASED ON ρ, v, μ AFTER SHOCK.

SECTION VII

CONCLUSIONS

The following conclusions may be drawn from the results of this study. It should be kept in mind that the basic underlying assumptions are that there is no heat transfer between the surface and the fluid and that the Prandtl number is equal to unity.

a) The previously known boundary layer growth due to compressibility is verified in this study.

b) Compressibility and Reynolds number effects for the ogive selected with no pressure gradient are consistent with the effects predicted by Emmons and Brainerd for the flat plate.

c) C_D values for the ogive selected with no pressure gradient are 10% higher than flat plate values in both the compressible and incompressible cases.

d) Pressure gradient effects are felt in two ways:

   1) There is an essential change in the velocity profile relation which causes an increase in C_D

   2) There is an increase in C_D due to the retardation of growth of the boundary layer.

e) The usual practice of applying incompressible flat plate C_D's to ogives in a supersonic stream or in incompressible flow is shown to be highly unconservative. (For the cases under consideration, the practice would result in an error of 35%.)

f) The practice of using the Blasius flat plate C_D values with Reynolds number based on the Reynolds number after shock to

represent the value of C_D, based on nose dynamic pressure, of the ogive in compressible flow with pressure gradient results in values approximately 35% unconservative.

SECTION VIII

REFERENCES

1. Emmons, H. W., and Brainerd, J. G., "Effect of Variable Viscosity on Boundary Layers, with a Discussion of Drag Measurements" A.S.M.E. Transactions, J. Applied Mechanics, 9, pA-1, (1942).
2. Busemann, A., "Gas - strömung mit laminaren Grenzschicht entlang einer Platt", ZAMM, 15, (1935).
3. Kármán, T. von, "The Problem of Resistance in Compressible Fluids", Proc. of Volta Congress, (1935).

3a. Illingworth, C. R., "The Laminar Boundary Layer Associated with the Retarded Flow of a Compressible Fluid", t.b.p.i. R.& M.

4. Mangler, W., "Compressible Boundary Layers on Bodies of Revolution", Captured German Document 496, Joint Intelligence Objectives Agency.
5. Hantzsche, W., and Wendt, H., "Laminar Boundary Layer at a Circular Cone with Zero Angle of Incidence in Supersonic Flow", Jahrb. (1941), d. Dt., Luftfahrtforschung.
6. Millikan, C. B., "The Boundary Layer and Skin Friction for a Figure of Revolution", A.S.M.E. Transactions, A.P.M. - 54 - 3, Vol. 54, (1932).
7. Keuthe, A. M., and Epstein, H. T., "Viscosity Effects in Transonic and Supersonic Flow", Bumblebee Series, Report No. 48, (December, 1946).
8. Classnotes taken in Dr. H. J. Stewart's course AE 258, at C.I.T., (1947).
9. Taylor, G. I., and Maccoll, J. W., "The Air Pressure on a Cone Moving at High Speed", Proceedings of The Royal Society, Series A, Vol. 139,

Jan. - Mar., (1933).

10. Prandtl, L., "The Mechanics of Viscous Fluids", Aerodynamic Theory, W. F. Durand, Ed., Vol. III, Springer, (1935).

11. Erdmann, "Pressure Distribution Measurements on an A4V1P in the Region of Sonic and Supersonic Velocities", Archive No. 66/100g. Kdes. Nov. 27, (1942). (Translation CGD 231).

12. Schubert, "The Axial Symmetric Flow Around the Body of the Missile A4 at Mach No. 1.87 and 1.56", Archive No. 66/101.

13. McAdams, W. H., "Heat Transmission", McGraw - Hill, (1942)

14. Allen, H. J., and Nitzberg, G. E., "The Effect of Compressibility on the Growth of the Laminar Boundary Layer on Low Drag Wings and Bodies", NACA ACR, Jan., (1943).

15. Bairstow, L., "Applied Aerodynamics", Longmans, (1939).

16. Liepmann, H. W., and Puckett, A. E., "Introduction to Aerodynamics of a Compressible Fluid", Wiley, (1947).

17. Prandtl, L., and Tietjens, O. G., "Fundamentals of Hydro and Aeromechanics", McGraw - Hill, (1934).

SECTION IX

COMPUTATIONS

EVALUATION OF BOUNDARY LAYER THICKNESS AND SKIN FRICTION DRAG COEFFICIENT

A.

Case I Compressible Flow with Pressure Gradient

Boundary Layer Thickness

The procedure for determining boundary layer thickness consists of the following steps:

1. Pressure distribution data as presented in Figure 3 is inserted into expressions (13a) and (13c). Resulting values are shown in Tables X and XI. The same values are shown plotted on Figures 6 and 7.

2. The curves on Figures 6 and 7 are then graphically integrated to give $F_1(s)$ and $F_2(s)$ of (13b) and 13d) respectively which are shown plotted versus P/P_o in Figure 8 and versus s in Figure 9.

3. The functions G(s) and H(s) of equation (16a) are then evaluated using the data obtained in step 2 above and equations (31) and (31a). These evaluations are shown in Tables (XII), (XIII) and (XIV) for $M = 1.87$.

4. Boundary layer thicknesses are then obtained by a numerical method of integration and the results are shown in Table VIII of the results.

FIG. 3 PRESSURE RATIO, P/P_0 VS S

$M = 1.87$

⊙ EXPERIMENTAL POINTS FROM REF. 12

—— $P/P_0 = 0.00575 + e^{-2.345\,S}$

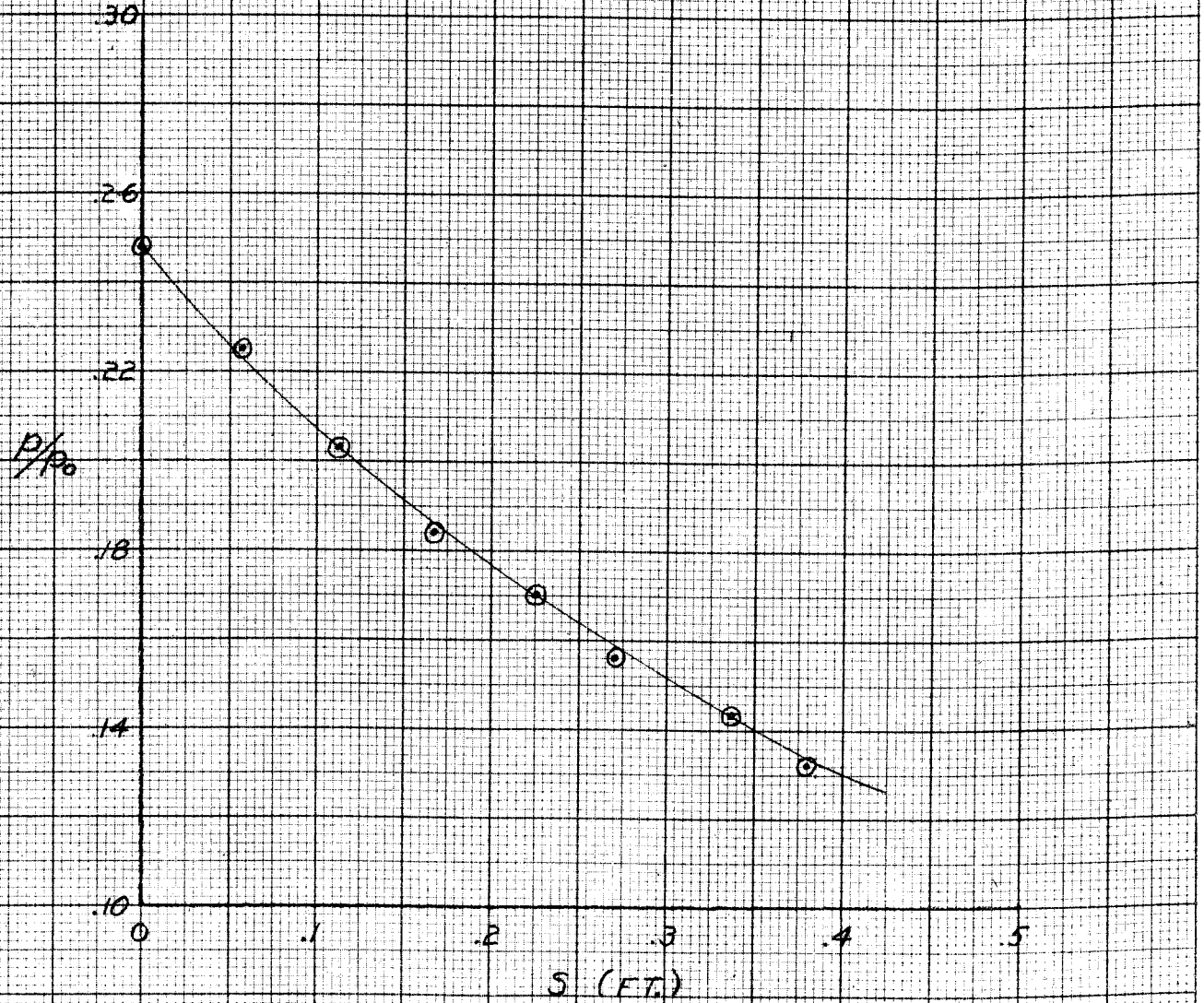

TABLE X $\qquad F_1(s) = \int_0^1 \frac{2P(s)\,\lambda(\eta)^2}{1 - P(s)\,\lambda(\eta)^2}\,d\eta$

P/P_o				.10		.16		.22		.28		.36	
$P(s)$				.4822		.4075		.351		.3052		.2532	
η	λ	λ^2		$P\lambda^2$	$d[F_1(s)]$	$P\lambda^2$	$d[F_1(s)]$	$P\lambda^2$	$d[F_1(s)]$	$P\lambda^2$	$d[F_1(s)]$	$P\lambda^2$	$d[F_1(s)]$
.1	.271	.07344		.035412	.0734	.02992	.0617	.02577	.0529	.022415	.04586	.01860	.0379
.2	.488	.23810		.11481	.2594	.09702	.2149	.08357	.1824	.07267	.1567	.06028	.1283
.4	.784	.61465		.29368	.8425	.25047	.6683	.21574	.5502	.18759	.4618	.15563	.3686
.6	.936	.87609		.42245	1.4629	.35700	1.1104	.30751	.8881	.26738	.7300	.22182	.5701
.8	.992	.98406		.47451	1.8060	.40100	1.3389	.34549	1.0553	.30034	.8585	.24916	.6637
1.0	1.000	1.0000		.48220	1.8625	.4075	1.3755	.35100	1.0817	.3052	.5330	.25320	.6781

TABLE XI $\qquad F_2(s) = \int_0^1 \frac{\sqrt{P(s)}\,\lambda(\eta)}{1 - P(s)\,\lambda(\eta)^2}\,d\eta$

P/P_o		.10		.16		.22		.28		.36	
$\sqrt{P(s)}$		.6945		.6386		.5933		.5520		.5030	
η		$\sqrt{P}\,\lambda$	$d[F_2(s)]$	$\sqrt{P}\,\lambda$	$d[F_2(s)]$	$\sqrt{P}\,\lambda$	$d[F_2(s)]$	$\sqrt{P}\,\lambda$	$d[F_2(s)]$	$\sqrt{P}\,\lambda$	$d[F_2(s)]$
.1		.18821	.19511	.17306	.1784	.16078	.1650	.14960	.1530	.13631	.1389
.2		.33892	.3829	.31164	.3451	.28953	.3159	.26937	.2905	.24546	.2612
.4		.5445	.7739	.50066	.6680	.46515	.5931	.43277	.5327	.39435	.4670
.6		.6501	1.1255	.59773	.9296	.55533	.8019	.51667	.7052	.47081	.6050
.8		.6889	1.3110	.63349	1.0576	.58855	.8991	.54758	.7826	.49898	.6646
1.0		.6945	1.3413	.6386	1.0778	.59330	.9142	.55200	.7945	.50300	.6735

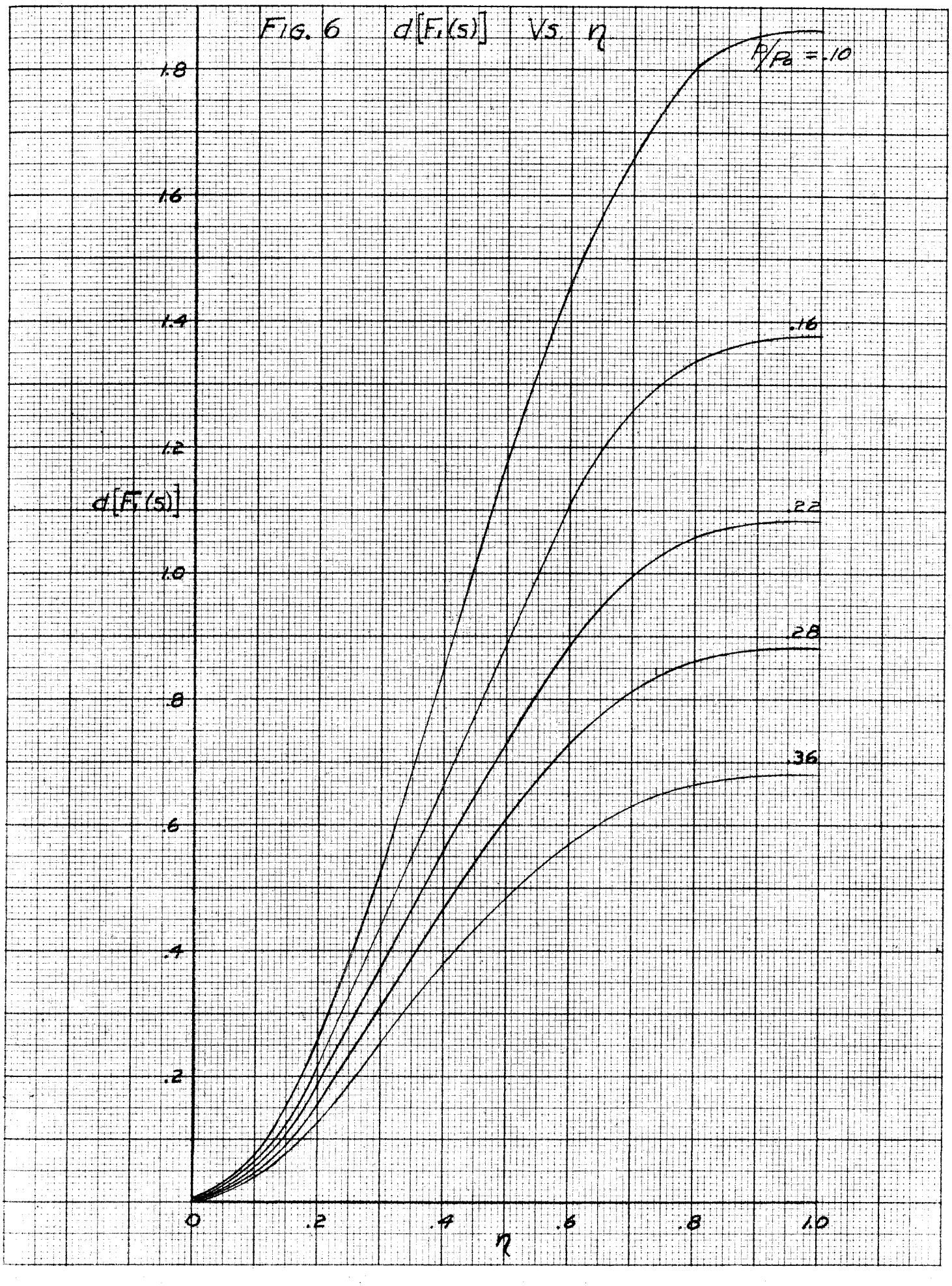
FIG. 6 d[F₁(s)] Vs. η
P/P₂ = .10
.16
.22
.28
.36
d[F₁(s)]
1.8
1.6
1.4
1.2
1.0
.8
.6
.4
.2
0
.2
.4
.6
.8
1.0
η

Fig. 7 $d[F_2(s)]$ Vs η

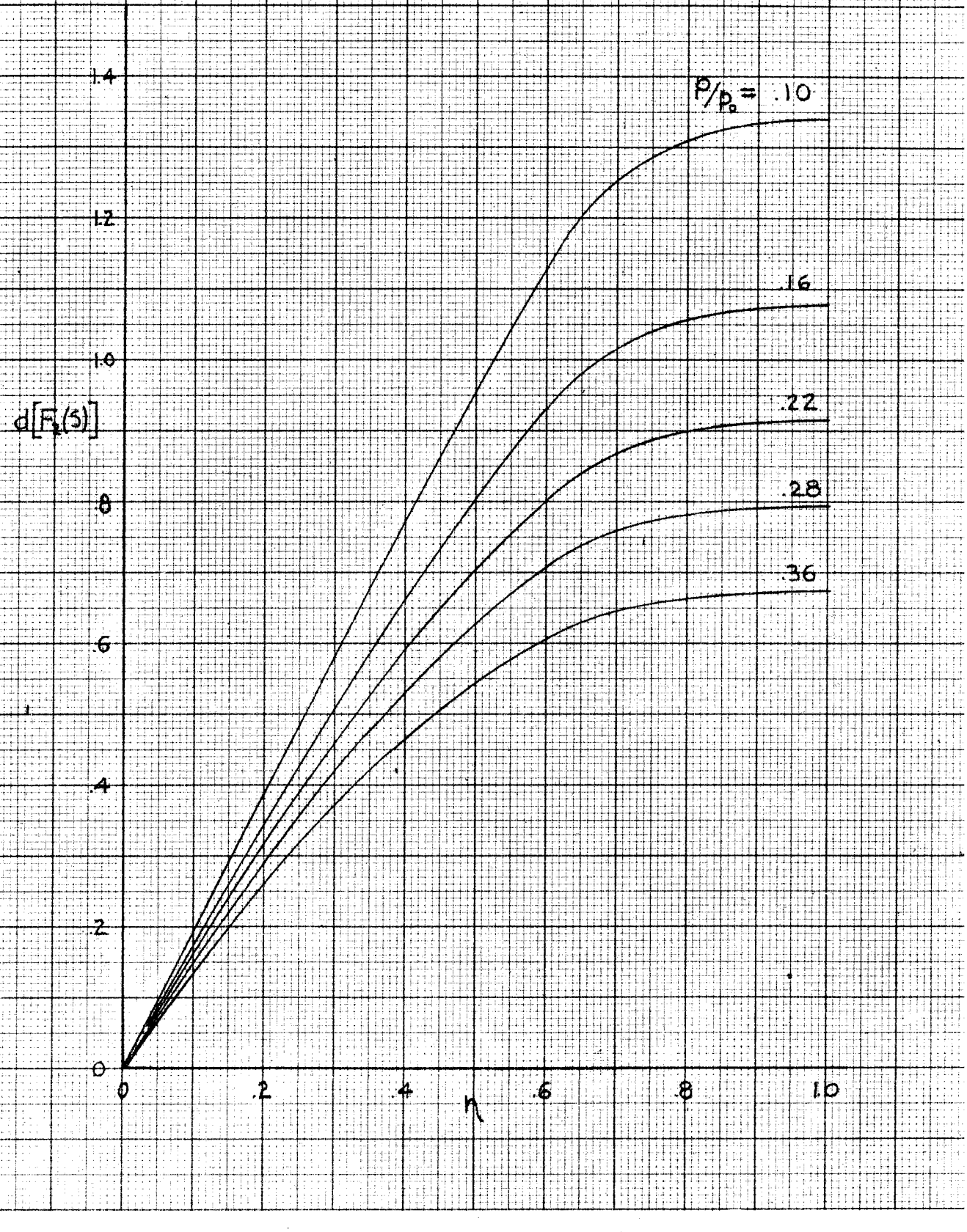

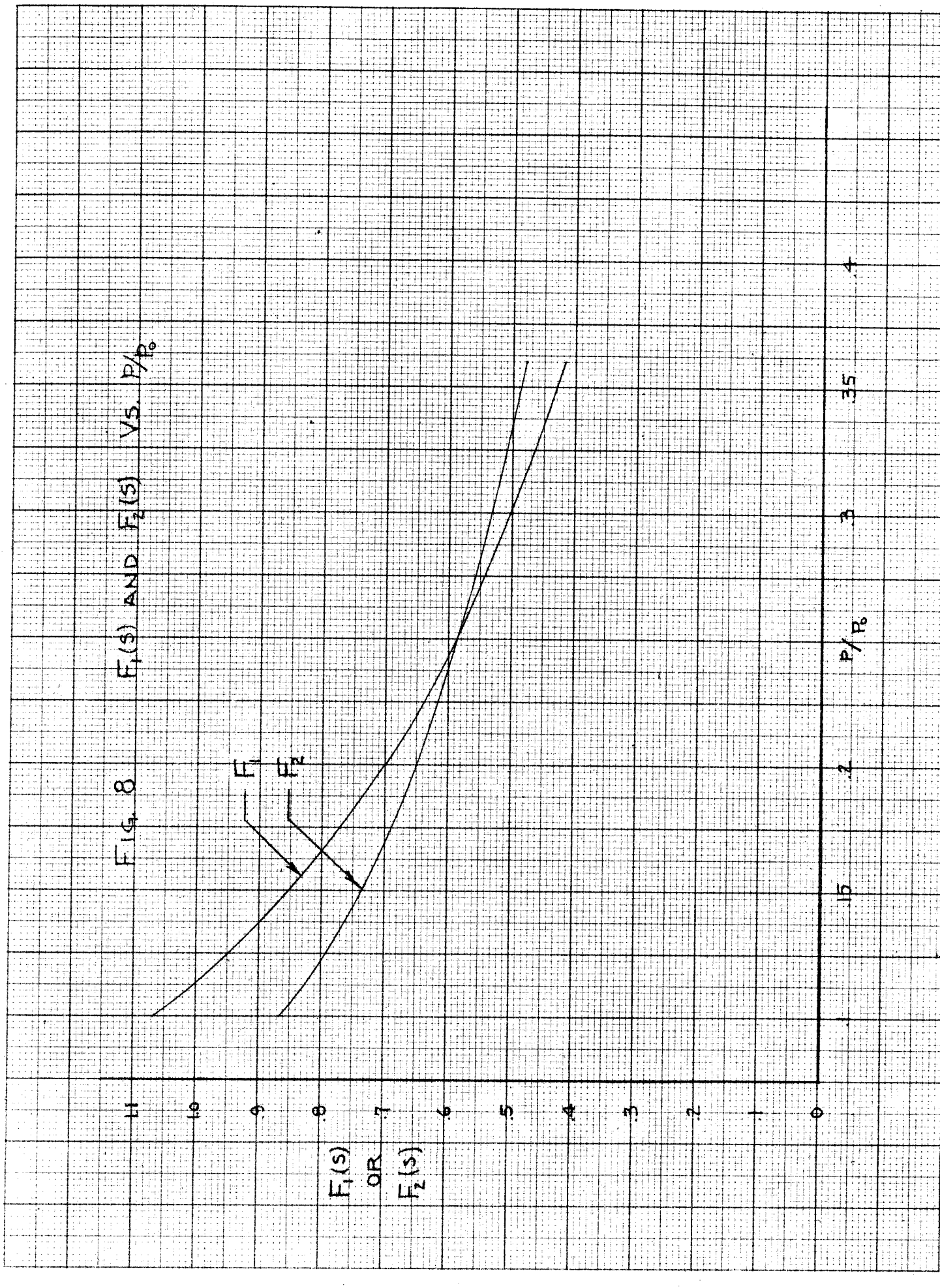
Fig. 8 $F_1(s)$ AND $F_2(s)$ VS. P/P_o
F_1
F_2
$F_1(s)$ OR $F_2(s)$
1.1
1.0
.9
.8
.7
.6
.5
.4
.3
.2
.1
0
.15
.2
.3
.35
.4
P/P_o

FIG. 9 $F_1(s)$ AND $F_2(s)$ VS s

$M = 1.87$

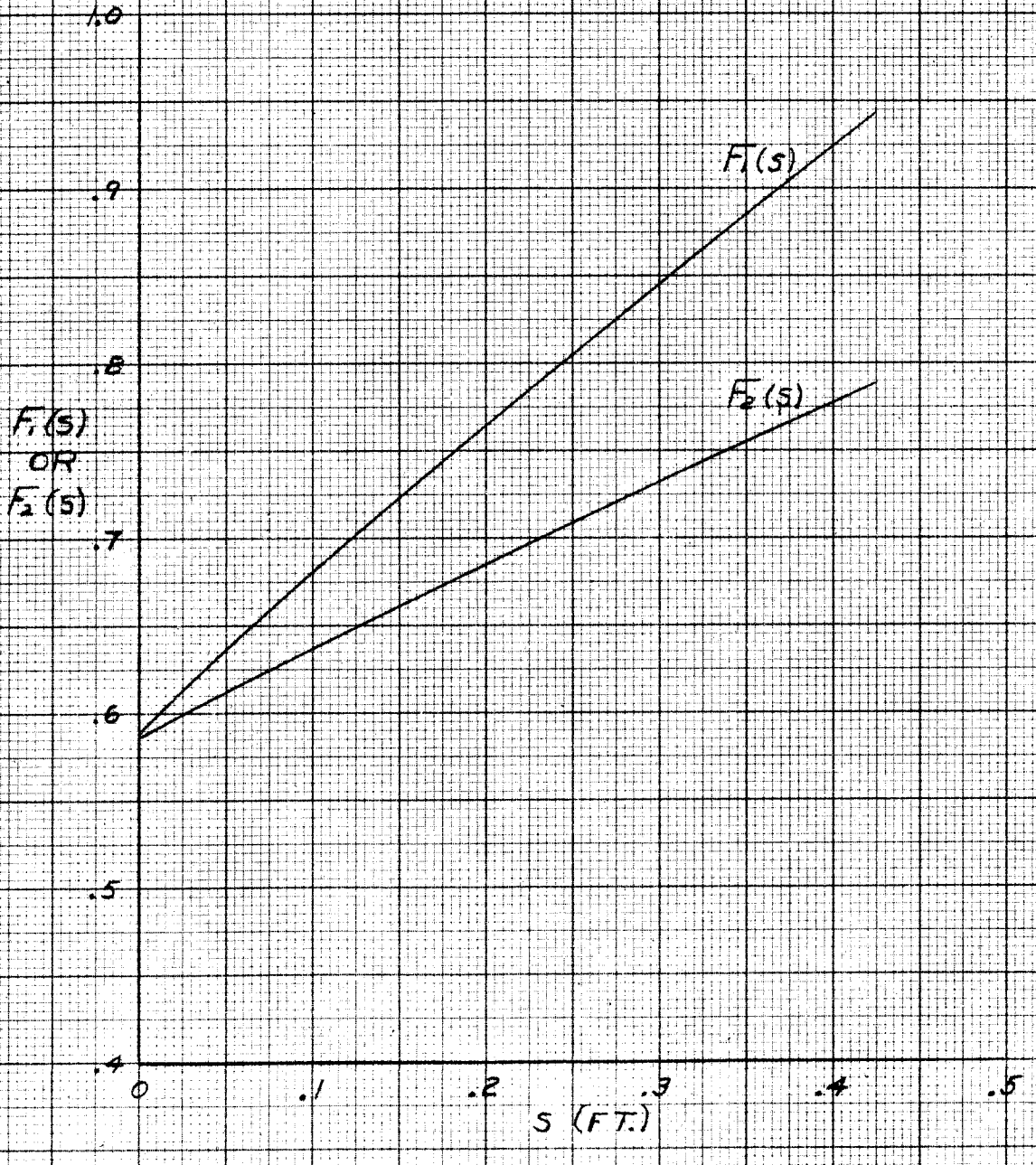

TABLE XII SECOND TERM IN NUMERATOR OF LAST TERM ON L.H.S. OF EQN. (16)

$$-v_{s_\delta}\sqrt{\frac{2}{C_p T_o}}\left\{\frac{d}{ds}(r_o p F_2)\right\} + r_o\left(\frac{\gamma-1}{\gamma}\right)\frac{dp}{ds}$$

$M = 1.87$

S	$\frac{p}{p_o}$	$\frac{1}{p_o}\frac{dp}{ds}$	F_2	$\frac{dF_2}{ds}$	r_o	$\frac{dr_o}{ds}$	$r_o p \frac{dF_2}{ds}$ (x10)	$pF_2\frac{dr_o}{ds}$ (x10)	$r_o F_2 \frac{dp}{ds}$ (x10)	{ } (x10)	$-v_{s_\delta}\{\}\sqrt{}$ (x10)	$r_o\left(\frac{\gamma-1}{\gamma}\right)\frac{dp}{ds}$ (x10)	SECOND TERM (x10)	NUMERATOR (x10)	H(s)
0.000	.248	-.451	.587	.520	.0000	.2902	.0000	.4225	-.0000	.4225	-.4840	-.0000	-.4840	-.0580	∞
.025	.237	-.424	.600	.518	.0060	.2733	.0074	.3890	-.0153	.3810	-.4420	-.0073	-.4493	-.0540	90.40
.050	.227	-.401	.613	.510	.0130	.2575	.0151	.3585	-.0266	.3470	-.4075	-.0149	-.4224	-.0500	40.30
.100	.208	-.357	.638	.500	.0244	.2230	.0254	.2960	-.0555	.2659	-.3190	-.0249	-.3439	-.0435	19.94
.150	.191	-.312	.662	.485	.0351	.1891	.0325	.2390	-.0725	.1990	-.2445	-.0313	-.2758	-.0353	11.83
.200	.176	-.282	.686	.465	.0434	.1546	.0356	.1867	-.0840	.1383	-.1730	-.0350	-.2080	-.0320	9.20
.250	.163	-.245	.709	.465	.0505	.1204	.0383	.1343	-.0877	.0899	-.1141	-.0354	-.1495	-.0257	6.54
.300	.151	-.223	.733	.465	.0560	.0857	.0394	.0948	-.0916	.0426	-.0550	-.0357	-.0907	-.0166	3.94
.350	.141	-.192	.756	.465	.0590	.0513	.0387	.0546	-.0855	.0078	-.0102	-.0323	-.0425	-.0100	2.32
.400	.131	-.178	.779	.465	.0607	.0168	.0370	.0171	-.0842	-.0301	.0399	-.0309	.0092	-.0067	1.57
.424	.127	-.167	.791	.465	.0610	.0000	.0360	.0000	-.0803	-.0443	.0581	-.0291	.0291	-.0065	1.52

TABLE XIII FIRST TERM IN NUMERATOR OF THE LAST TERM ON L.H.S. OF (16), $\frac{d}{ds}(r_0 p F_1)$ M = 1.87

S	$\frac{P}{P_0}$	$e^{-2.3455}$	$\frac{1}{P_0}\frac{dp}{dS}$	F_1	$\frac{dF_1}{dS}$	r_0	$\frac{dr_0}{dS}$	$r_0 p \frac{dF_1}{ds}$	$pF_1\frac{dr_0}{dS}$	$r_0 F_1 \frac{dp}{ds}$	$\frac{1}{P_0}\frac{d(r_0 p F_1)}{ds}$
0	.248	1	−.451	.589	.980	0	.2902	0	.0424	0	.0424
.025	.237	.940	−.424	.613	.965	.0065	.2733	.00137	.0414	−.00156	.0412
.050	.227	.889	−.401	.637	.935	.0130	.2575	.00276	.0372	−.00332	.0366
.100	.208	.791	−.357	.682	.875	.0244	.2230	.00444	.0316	−.00593	.0302
.150	.191	.693	−.312	.724	.845	.0351	.1891	.00566	.0262	−.00793	.0239
.200	.176	.625	−.282	.766	.820	.0434	.1546	.00626	.0208	−.00939	.0175
.250	.163	.543	−.245	.806	.795	.0505	.1204	.00653	.0158	−.00997	.0124
.300	.151	.495	−.223	.846	.785	.0560	.0857	.00664	.0110	−.01057	.0070
.350	.141	.425	−.192	.886	.775	.0590	.0513	.00645	.00641	−.01001	.0029
.400	.131	.395	−.178	.925	.768	.0607	.0167	.00611	.00203	−.0100	−.0019
.424	.127	.370	−.167	.944	.765	.0610	0	.00593	0	−.00959	−.0037

TABLE XIV DENOMINATORS FOR (16) FOR L.H.S. = $\frac{r_0 P}{2P_0}\left[F_1 - v_{s_\delta}\sqrt{\frac{2}{C_p T_0}}F_2\right]$; FOR R.H.S. = $\frac{\delta P}{2(\delta-1)}\left[F_1 - v_{s_\delta}\sqrt{\frac{2}{C_p T_0}}F_2\right]$

	①	②	③	④	⑤	⑥	⑦	⑧	⑨	⑩		⑪
S	$\sqrt{1-\frac{T}{T_0}}$	v_{s_δ}	$\sqrt{\frac{2}{C_p T_0}}v_{s_\delta}$	F_2	③×④	F_1 − ⑤	$\frac{1}{2}\frac{P}{P_0}$	DEN. L.H.S. = r_0 ⑥ ⑦	DEN. R.H.S. $\frac{}{r_0}$ = $\frac{\delta}{\delta-1}$ ⑥ ⑦	$\frac{3\mu_0 v_{s_\delta}}{P_0}$		G(S) − $\frac{⑩}{⑨}$
								10^{-4}		10^{-7}		10^{-5}
0	.573	1442	1.146	.587	.672	−.083	.1240	0	−.0360	3.945		1.097
.025	.580	1460	1.160	.600	.696	−.084	.1185	−.597	−.0351	3.995		1.140
.050	.588	1479	1.174	.613	.720	−.084	.1135	−1.240	−.0334	4.045		1.212
.100	.601	1512	1.201	.638	.766	−.086	.1040	−2.183	−.0313	4.140		1.321
.150	.614	1544	1.228	.662	.814	−.089	.0955	−2.985	−.0298	4.225		1.420
.200	.626	1575	1.251	.686	.857	−.091	.0880	−3.430	−.0280	4.310		1.539
.250	.636	1600	1.271	.709	.901	−.096	.0815	−3.930	−.0273	4.380		1.607
.300	.646	1627	1.292	.733	.946	−.0996	.0755	−4.210	−.0263	4.450		1.693
.350	.654	1648	1.309	.756	.990	−.1038	.0705	−4.320	−.0256	4.510		1.762
.400	.663	1669	1.326	.779	1.032	−.1076	.0655	−4.280	−.0249	4.565		1.833
.424	.667	1680	1.335	.791	1.055	−.1105	.0635	−4.280	−.0245	4.600		1.849

INTEGRATION OF THE BOUNDARY LAYER EQUATION

The boundary layer equation is of the form:

$$\frac{dy}{ds} = G(s) - y\,H(s)$$

where $y = \delta^2$

$$F(s) = \frac{\frac{d}{ds}\left[r_o \frac{p}{p_o} F_1(s)\right] - v_{s_\delta}\sqrt{\frac{2}{C_p T_o}}\frac{d}{ds}\left[r_o \frac{p}{p_o} F_2(s)\right]\frac{\gamma-1}{\gamma} r_o \frac{d(\frac{p}{p_o})}{ds}}{\frac{1}{2} r_o \frac{p}{p_o}\left[F_1(s) - \sqrt{\frac{2}{C_p T_o}}\, v_{s_\delta}\, F_2(s)\right]}$$

$$G(s) = \frac{-3\mu_o v_{s_\delta}}{\frac{1}{2}\frac{\gamma}{\gamma-1} p\left[F_1(s) - \sqrt{\frac{2}{C_p T_o}}\, v_{s_\delta}\, F_2(s)\right]}$$

The above equation can be integrated rather quickly using Adams Method.

$$y_{n+1} = y_n + h\left[q_n + \tfrac{1}{2}\Delta q_{n-1} + \frac{5}{12}\Delta^2 q_{n-2} + \frac{3}{8}\Delta^3 q_{n-3} + \ldots\right]$$

where $h = s_{n+1} - s_n$

$$q = \frac{dy}{ds}$$

$\Delta^n = n^{th}$ differende.

Here, the three point formula is used taking $h = 0.025$ ft.

then $y_{n+1} = y_n + 0.025\left[q_n + \frac{1}{2}\Delta q_{n-1} + \frac{5}{12}\Delta^2 q_{n-2}\right]$

To start the numerical integration procedure, the solution, y and the slope must be known at three consectutive points. The slope, $(\frac{dy}{ds})_o$,

at the ogive nose, is determined from the differential equation assuming that the boundary layer thickness at the nose is zero.

The boundary layer equation is:

$$\frac{dy}{ds} + y \left\{ \frac{\frac{d}{ds}\left[r_o \, p/p_o \, F_1(s)\right] - v_{s_\delta} \sqrt{\frac{2}{C_p T_o}} \frac{d}{ds}\left[r_o \frac{p}{p_o} F_2(s)\right] + \frac{\gamma - 1}{\gamma} r_o \frac{d(p/p_o)}{ds}}{\frac{1}{2} r_o \, p/p_o \left[F_1(s) - \sqrt{\frac{2}{C_p T_o}} v_{s_\delta} \; F_2(s)\right]} \right\}$$

$$= \frac{-3 \mu_o v_{s_\delta}}{\frac{1}{2} \frac{\gamma}{\gamma - 1} p \left[F_1(s) - \sqrt{\frac{2}{C_p T_o}} \; v_s \quad F_2(s)\right]}$$

As $s \to 0$, $r_o \to 0$ and $y \to 0$. Hence the second term on the R.H.S. of the above equation take the indeterminant form $\frac{0}{0}$. By taking derivatives of the numerator and the denominator of this term, the limit as $s \to 0$ can be found.

Then at $s = 0$ the boundary layer equation is of the form:

$$\left(\frac{dy}{ds}\right)_o + K \left(\frac{dy}{ds}\right)_o = G(s)_o$$

Using values of K and $G(s)_o$ determined from tables X II and XIII,

$$\left(\frac{dy}{ds}\right)_{M = 1.56} = 0.5310 \times 10^{-5} \text{ ft.}$$

$$\left(\frac{dy}{ds}\right)_{M = 1.87} = 0.6940 \times 10^{-5} \text{ ft.}$$

To determine the solution and slopes at $s = 0.025$ ft. and $s = 0.050$ ft. a Taylor expansion is used as follows:

$$y_{n+1} = y_n + \left(\frac{dy}{ds}\right)_n \Delta s + \frac{1}{2} \left(\frac{d^2y}{ds^2}\right)_n (\Delta s)^2 + \cdots\cdots$$

$$\text{Let} \quad \left(\frac{d^2y}{ds^2}\right)_n = \frac{\left(\frac{dy}{ds}\right)_{n+1} - \left(\frac{dy}{ds}\right)_n}{\Delta s}$$

$$\text{Also} \quad \left(\frac{dy}{ds}\right)_{n+1} = G_{n+1}(s) - y_{n+1} H_{n+1}(s)$$

$$\text{Then} \quad \left(\frac{d^2y}{ds^2}\right)_n = \frac{G_{n+1}(s) - y_{n+1} H_{n+1}(s) - \left(\frac{dy}{ds}\right)_n}{\Delta s}$$

Therefore,

$$y_{n+1} = \frac{1}{1 + \frac{G_{n+1}(s)\Delta s}{2}} \left\{ y_n + \frac{\Delta s}{2} \left[\left(\frac{dy}{ds}\right)_n + G_{n+1}(s) \right] \right\}$$

Using this method, the solution is determined at $s = 0.025$ and $s = 0.050$.

Now, having the solution and the slope at three consectutive points, the remaining solution is determined using Adam's Method. (Table XV).

TABLE XV INTEGRATION OF THE BOUNDARY LAYER EQUATION, M = 1.87

						A	B	C	D	E							
S	y $\times 10^{8}$	q $\times 10^{5}$	Δq $\times 10^{5}$	$\Delta^2 q$ $\times 10^{5}$	y_n $\times 10^{8}$	q_n $\times 10^{5}$	$\frac{1}{2} q_{n+1}$ $\times 10^{5}$	$\frac{5}{12}\Delta^2 q_{n+1}$ $\times 10^{5}$	B+C+D $\times 10^{5}$	0.025 E $\times 10^{8}$	y_{n+1} $\times 10^{8}$	G_{n+1} (S) $\times 10^{5}$	H_{n+1} (S)	$y_{n+1} G_{n+1}$ (S) $\times 10^{5}$	q_{n+1} $\times 10^{5}$	δ $\times 10^{4}$
0.000	00.00	0.6440										2.041	∞			0.00
			.0410													
.025	15.58	.7350		.0510								2.140	90.40			3.94
			.0920													
.050	35.10	.8270		-.1390								2.240	40.30			5.93
			-.0470													
.075	57.45	.7800		.2130	35.10	.827	.0460	.0212	.8942	22.35	57.45	2.340	27.20	1.560	.780	7.59
			.1660													
.100	74.90	.9460		-.1650	57.45	.780	-.0235	-.0579	.6986	17.45	74.90	2.440	19.94	1.494	.946	8.65
			.0010													
.125	102.80	.9470		.2020	74.90	.946	.0830	.0880	1.1170	27.90	102.80	2.539	15.50	1.592	.947	10.28
			.2030													
.150	124.80	1.1500		.2720	102.80	.947	.0005	-.0686	.8790	22.00	124.80	2.630	11.83	1.480	1.150	11.19
			-.0690													
.175	158.07	1.0810		.3420	124.80	1.150	.1015	.0840	1.3355	33.27	158.07	2.725	10.40	1.644	1.081	12.59
			.0700													
.200	181.37	1.1510		.1690	158.07	1.081	-.0345	-.1130	.9335	23.30	181.37	2.820	9.30	1.669	1.151	13.47
			.2390													
.225	217.07	1.3900		-.2990	181.37	1.151	.0350	.1420	1.4280	35.70	217.07	2.910	7.00	1.520	1.390	14.74
			-.0600													
.250	256.57	1.3100		.3650	217.07	1.390	.1195	.0705	1.5800	39.50	256.57	2.990	6.54	1.680	1.310	16.02
			.3050													
.275	285.45	1.6150		-.0860	256.57	1.310	-.0300	.1245	1.4550	28.88	285.45	3.070	5.10	1.455	1.615	16.90
			.2190													
.300	332.05	1.8340		-.0120	285.45	1.615	.1025	.1520	1.8695	46.60	332.05	3.144	3.94	1.310	1.834	18.20
			.2070													
.325	379.65	2.0410		.0270	332.05	1.834	.1095	-.0358	1.9077	47.60	379.65	3.216	3.10	1.175	2.041	19.50
			.2340													
.350	433.15	2.2750		-.1040	379.65	2.041	.1035	-.0050	2.1395	53.50	433.15	3.280	2.32	1.005	2.275	20.80
			.1300													
.375	493.15	2.4050		-.0120	433.15	2.275	.1175	.0120	2.4082	60.00	493.15	3.341	1.90	.936	2.405	22.20
			.1180													
.400	553.75	2.5230			493.15	2.405	.0650	-.0434	2.4266	60.60	553.75	3.393	1.57	.870	2.523	23.55
.425	618.15				553.75	2.523	.0590	-.0050	2.5710	64.40	618.15	3.440	1.52	.939	2.501	24.85

Skin Friction Drag Coefficient

The differential of equation (28) is evaluated using the results of step 4 above and data contained in Table XV.

This is shown plotted versus s for $M = 1.87$ in Figure 10. By a graphical integration the axial drag force is evaluated and put into coefficient form through equations (29) and (30).

For $M = 1.87$

$$q = \frac{\gamma}{2} P M^2$$

$$= .7(350)\ (1.87)^2 = 857 \text{ lb} - \text{ft}^{-2}$$

The resulting drag coefficients are presented in Table IX of the results.

TABLE XVI ITEM FOR USE IN EVALUATION OF DRAG FOR CASE I, M=1.87

$$D = 6\pi\mu_0 \int_0^{s=.424} \frac{v_{s_\delta} r_0 \cos\beta}{\delta}\, ds$$

s	$r_0 \cos\beta$	δ	$\frac{r_0 \cos\beta}{\delta}$	v_{s_δ}	$v_{s_\delta}\frac{r_0 \cos\beta}{\delta}$
	$\times 10^4$	$\times 10^4$			$\times 10^{-3}$
0	00.0	0.00	—	1442	—
.025	62.4	3.94	15.83	1460	23.10
.050	116.3	5.93	19.63	1479	29.00
.100	238.0	8.65	27.50	1512	41.60
.150	345.0	11.19	30.84	1544	47.60
.200	429.0	13.47	31.83	1575	50.10
.250	501.0	16.02	31.30	1600	50.90
.300	558.0	18.20	30.63	1627	49.80
.350	589.0	20.80	28.30	1648	46.60
.400	607.0	23.55	25.82	1669	43.10
.424	610.0	24.85	2455	1680	41.20

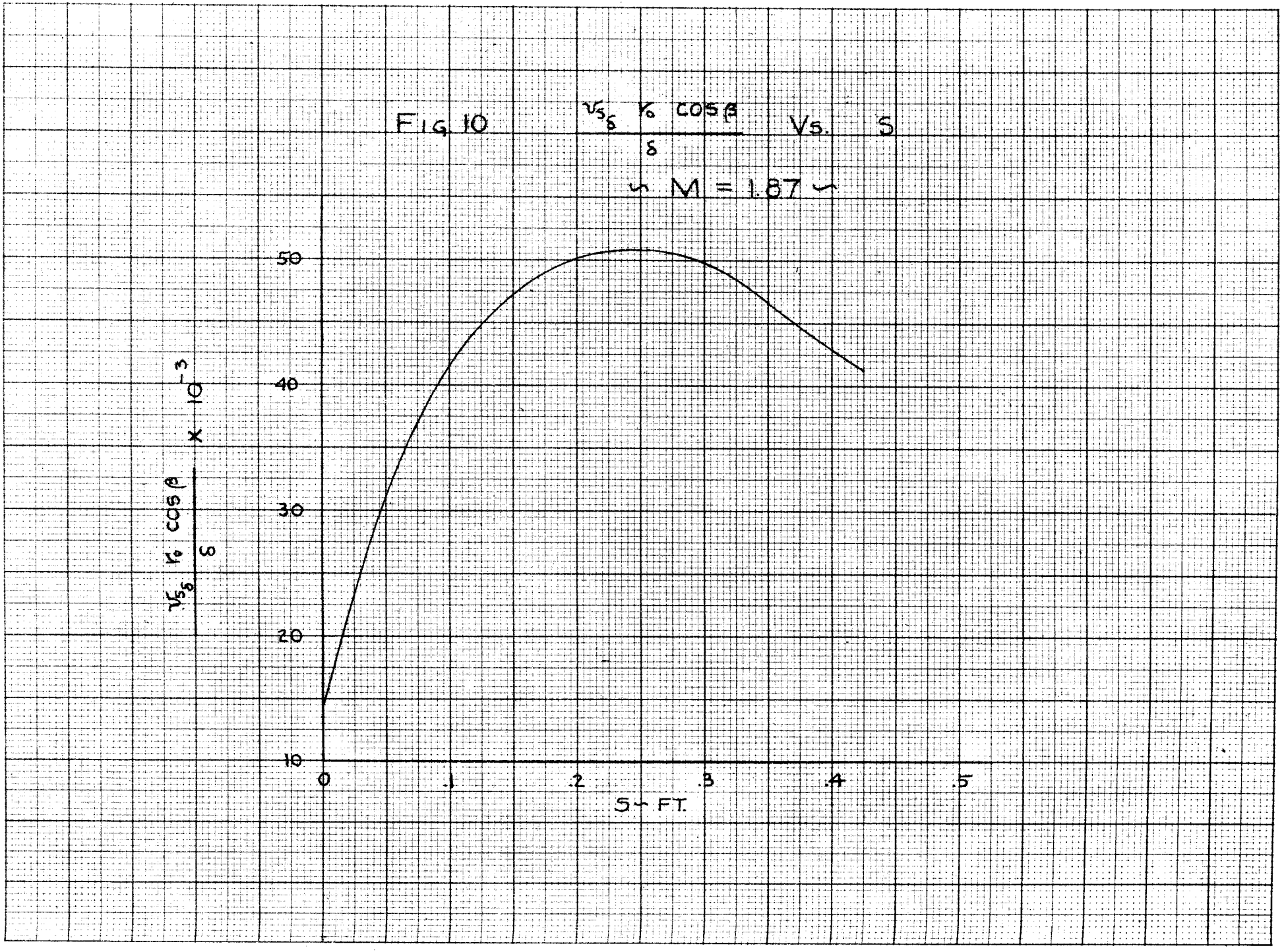
FIG. 10 v_{s_δ} $r_0 \cos\beta$ / δ VS. S
M = 1.87
v_{s_δ} $r_0 \cos\beta$ / δ x 10^{-3}
50
40
30
20
10
0
.1
.2
.3
.4
.5
S → FT.

Evaluation of C_D ($M_\infty = 1.87$)

$$D = 6\pi \mu_o \int_o^{s=0.424} \frac{v_{s_\delta} \; r_o \cos\beta}{\delta} \, ds$$

$$\int_o^{s=0.424} \frac{v_{s_\delta} \; r_o \cos\beta}{\delta} \, ds = 17.51 \times 10^3 \qquad \text{(Graphical Integration)}$$

$$\mu_o = 3.76 \times 10^{-7} \quad \text{slugs} - \text{ft.}^{-1} - \text{sec.}^{-1}$$

$D = 0.1239$ lbs.

$q = 857$ lb. - ft.$^{-2}$ $\qquad A = 0.1089$ ft.^{2} (wetted area)

$C_D = 0.001328$

Case II Compressible Flow with No Pressure Gradient

Boundary Layer Thickness

Values of the constant K of equation (17c) are obtained for two values of v_s comparable to free stream and nose value of pressure ratios.

$$\delta^2 = K \frac{\int_o^s r_o^2 \, ds}{r_o^2} \qquad (17c)$$

$$\text{where } K = \frac{-6 \mu_o v_{s_\delta}}{\frac{\gamma}{\gamma - 1} p \left(C_1 - v_{s_\delta} \sqrt{\frac{2}{C_p T_o}} C_2\right)}$$

Data are presented for $M = 1.87$; P/P_o = free stream value = 0.159

$$\begin{aligned} v_{s_\delta} &= 1610 \text{ ft.} - \text{sec.}^{-1} \\ p^{s_\delta} &= 350 \text{ lb.} - \text{ft.}^{-2} \\ \mu_o &= 3.76 \times 10^{-7} \text{ slug} - \text{ft.}^{-1} \text{ sec.}^{-1} \end{aligned}$$ from table VII

$$C_1 - v_{s_\delta} \sqrt{\frac{2}{C_p T_o}} C_2 = -0.0965$$ from Figure 8

$$\text{then } K = 3.075 \times 10^{-5}$$

$$\text{and } \delta^2 = 3.075 \times 10^{-5} \frac{\int_o^s r_o^2 \, ds}{r_o^2}$$

$\frac{\int_o^s r_o^2 \, ds}{r_o^2}$ appears in table XIX.

The boundary layer thickness is evaluated as

s(ft.)	δ (ft.) 10^{-3}
0	0
.025	0.557
.05	0.743
.10	1.069
.15	1.301
.20	1.546
.25	1.767
.30	1.980
.35	2.245
.40	2.500
.424	2.630

Skin Friction Drag Coefficient.

For this case equation (28) may be rewritten since v_{s_δ} is now a constant.

$$\text{Drag} = 6\pi\mu_o v_{s_\delta} \int_o^s \frac{r_o \cos\beta}{\delta} \, ds$$

for the above δ's s	$\frac{r_o \cos\beta}{\delta}$
0	-
.025	11.20
.05	15.67
.10	22.25
.15	26.50
.20	27.80
.25	28.30
.30	28.20
.35	26.25
.40	24.30
.424	23.20

This variation is graphically integrated to give

$$\int_o^s \frac{r_o \cos\beta}{\delta} \, ds = 9.648$$

$$6\pi\mu_o v_{s_\delta} = 6\pi \, 3.76 \times 10^{-7} \times 1610 = 11.41 \times 10^{-3}$$

$$\text{Drag} = 9.648 \times 11.41 \times 10^{-3} = .1100 \text{ lbs.}$$

$$q = \frac{\gamma}{2} p_\infty M_\infty^2 = .7\,(350)\,(1.87)^2 = 857 \text{ lb} - \text{ft.}^{-2}$$

$$A = .1089 \text{ ft.}^2$$

$$C_D = \frac{D}{q\,A}$$

$$= \frac{.1100}{857\,(.1089)}$$

$$= .001179$$

Case III Incompressible Flow with Pressure Gradient

Values for use in determination of boundary layer thickness from equation (23) are shown in Table XVII and are plotted versus s in Figure 11 for the case comparable to M = 1.87. The indicated integration is carried out by graphical means and the resulting boundary layer thicknesses are presented in the Table VIII.

TABLE XVII INCOMPRESSIBLE FLOW WITH PRESSURE GRADIENT ~ M = 1.87

$$\delta^2 = \frac{56.1\,\nu_0}{(r_0\,v_{s_\delta})^2\left(\frac{v_s^2}{2}\delta-\right)^{3.34}} \int_0^s \left\{ \frac{(r_0\,v_{s_\delta})^2 \left(\frac{v_s^2}{2}\delta-\right)^{3.34}}{v_{s_\delta}} \right\} ds$$

①	②	③	④	⑤	⑥	⑦	⑧	⑨	⑩	⑪	⑫	⑬		
s	r_0	P/P_0	1 − ③	$\sqrt{④}$	v_{s_δ}	② × ⑥	⑦²	$v_{s_\delta}^3/2$	⑨^3.34	⑧ × ⑩	⑪ / ⑥	$\int$ ⑫ ds	δ^2	δ
					10^3			10^6	10^{20}	10^{23}	10^{20}	10^{20}	10^{-6}	10^{-3}
0	0	.248	.752	.867	4.21	0	0	8.86		0	0	0	0	0
.025	.0065	.237	.763	.874	4.25	25.5	650.3	9.03	1722	1191	280	3	.150	.385
.050	.0130	.227	.773	.879	4.28	55.6	3091	9.16	1789	5525	1291	22.5	.243	.493
.100	.0244	.208	.792	.890	4.33	105.5	11,110	9.35	1965	21,820	5040	172.3	.471	.686
.150	.0351	.191	.809	.900	4.38	153.5	23,550	9.56	2050	48,300	11,040	559	.691	.831
.200	.0434	.176	.824	.908	4.41	191.5	36,570	9.72	2180	79,700	18,100	1284	.960	.981
.250	.0505	.163	.837	.915	4.45	225.0	50,625	9.90	2320	117,500	26,400	2404	1.220	1.104
.300	.0560	.151	.849	.922	4.49	251.5	63,250	10.08	2455	155,300	34,600	3937	1.510	1.229
.350	.0590	.141	.859	.927	4.51	266.0	70,756	10.17	2520	178,100	39,500	5802	1.940	1.393
.400	.0607	.131	.869	.932	4.53	275.0	75,625	10.26	2620	198,000	43,600	7890	2.375	1.541
.424	.0610	.127	.873	.935	4.54	277.0	76,729	10.31	2640	202,500	43,600	8944	2.630	1.622

NOTE: THE ABOVE VALUES WERE COMPUTED ON THE BASIS OF A HIGHER P_0 BUT AT CONSISTENT VALUES OF REYNOLDS NUMBER AND PRESSURE RATIOS, RESULTING IN IDENTICAL VALUES FOR δ AND C_D AS FOR THE CORRECT P_0.

FOR THE ABOVE TABLE $v_{s_\delta} = 4.86 \times 10^3 \sqrt{1 - P/P_0}$ AND $\nu_0 = \frac{\mu}{\rho} = \frac{3.76 \times 10^{-7}}{3.54 \times 10^{-4}} = 1.061 \times 10^{-3}$.

FIG. 11 INTEGRATION OF BOUNDARY LAYER EQ'N.
INCOMPRESSIBLE CASE; PRESSURE GRAD.

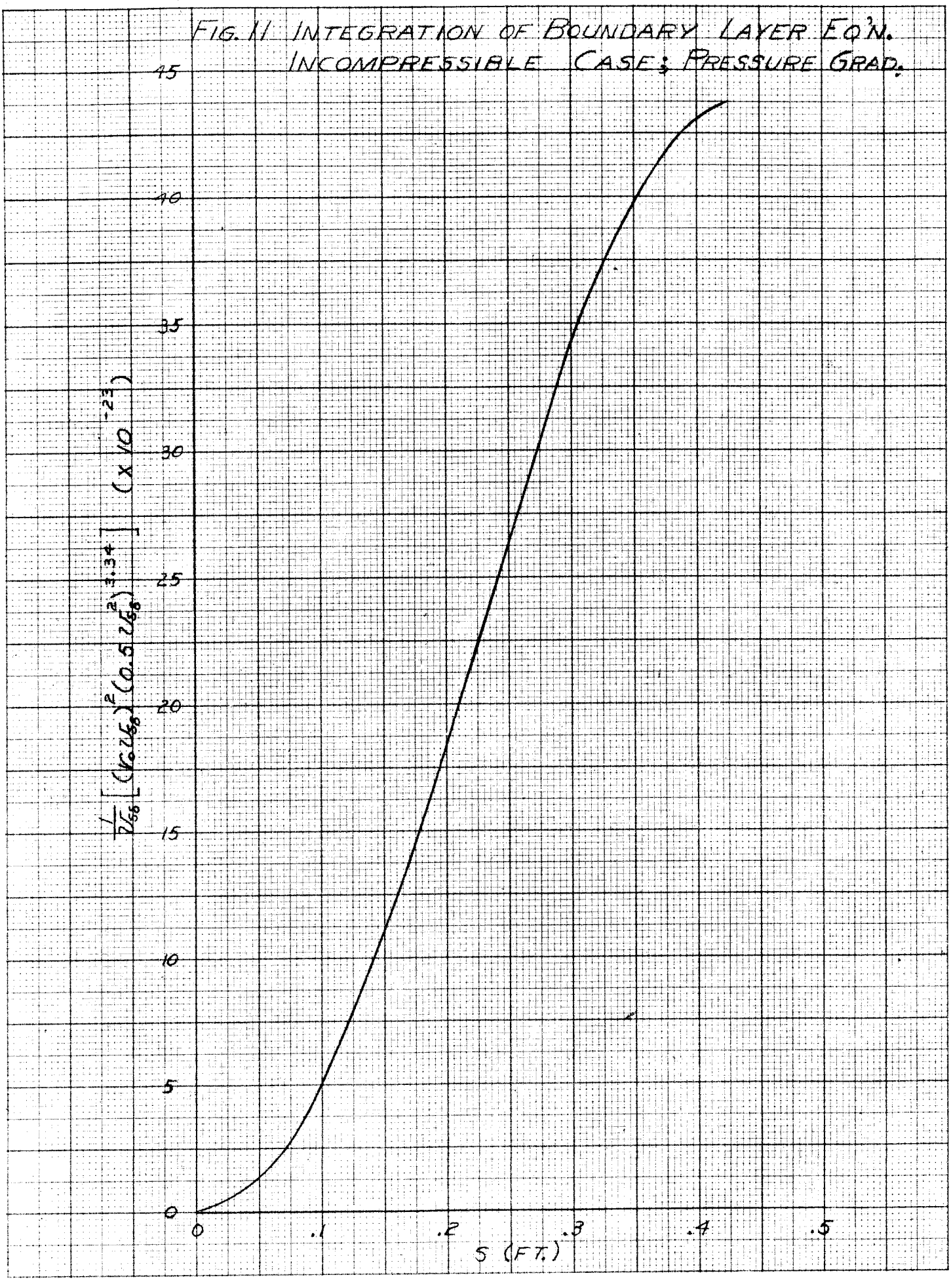

The skin friction drag coefficient is obtained as follows:

$$D = 6\pi\mu_o \int_o^s v_{s_\delta} \frac{r_o}{\delta} \cos\beta \; ds \qquad (28)$$

s	δ x 10^3	v_{s_δ} x 10^{-3}	$r_o \cos\beta$	$\frac{r_o \cos\beta}{\delta}$	$v_{s_\delta} \frac{r_o \cos\beta}{\delta}$ x 10^{-3}
0	0	4.21	0	-	-
0.025	0.387	4.25	0.00624	16.17	69
.050	.493	4.28	.01163	23.6	110
.100	.686	4.33	.0238	34.7	150
.150	.831	4.38	.0345	41.6	182
.200	.981	4.41	.0429	43.6	192
.250	1.104	4.45	.0501	45.4	202
.300	1.229	4.49	.0558	45.5	204
.350	1.393	4.51	.0589	42.2	191
.400	1.541	4.53	.0607	39.4	178
.424	1.622	4.54	.0610	37.6	171

By graphical integration $\int_o^s v_{s_\delta} \frac{r_o}{\delta} \cos\beta \; ds = 71.6 \times 10^3$ ft.^{2}/sec.

$6\pi\mu_o = 6\pi \times 3.76 \times 10^{-7} = 71 \times 10^{-1}$

$D = 0.508$ lb.

$v_\infty = 4460$ ft./sec.

$\rho_\infty = 3.54 \times 10^{-4}$ slugs/ft.^{3}

$q_\infty = \frac{1}{2} \rho_\infty v_\infty^2 = 3520$ lb./ft.^{2}

$A = 0.1089$ ft.^{2} (wetted area)

$$C_D = \frac{D}{q_\infty A} = \frac{.508}{3520 \times .1089}$$

$C_D = 0.00133$

$RN = 1.743 \times 10^6$

Case IV Incompressible Flow with No Pressure Gradient

The boundary layer thicknesses are evaluated for the case comparable to $M = 1.87$ with the free stream value of pressure ratio.

Data for equation (26)

$$p/p_o = \text{free stream} = .159$$

$$v_{s_\delta} = 2340 \text{ ft.} - \text{sec.}^{-1}$$

$$\nu_o = \frac{\mu}{\rho} = \frac{3.76 \times 10^{-7}}{6.77 \times 10^{-4}} = .555 \times 10^{-3}$$

$$\delta^2 = \frac{56.1\,(.555 \times 10^{-3})}{2340 \times 10^3} \quad \frac{\int_o^s r_o^2\, ds}{r_o^2}$$

$$= 1.330 \times 10^{-5} \quad \frac{\int_o^s r_o^2\, ds}{r_o^2}$$

s(ft)	δ (ft)
0	0
.025	.367
.05	.489
.10	.705
.15	.856
.20	1.013
.25	1.158
.30	1.300
.35	1.475
.40	1.645
.424	1.682

Skin Friction Drag Coefficient

$$D = 6\pi\mu_o v_{s_\delta} \int_o^s \frac{r_o \cos\beta}{\delta} ds$$

$$6\pi\mu_o v_{s_\delta} = 6\pi\ 3.76 \times 10^{-7} \times 4460 = 1.66 \times 10^{-2}$$

s	$\frac{r_o \cos\beta}{\delta}$
.0	-
.025	17.07
.05	23.75
.10	33.70
.15	40.30
.20	42.20
.25	43.20
.30	42.70
.35	39.90
.40	36.90
.424	36.20

$$\int_o^s \frac{r_o \cos\beta}{\delta} ds = 15.3$$

$$D = .254 \text{ lbs.}$$

$$q = \frac{1}{2}\rho v_{s_\delta}^2$$

$$= \frac{6.77 \times 10^{-4}}{2} (2340)^2 = 18.5 \times 10^2 \text{ lb.} - \text{ft.}^{-2}$$

$$A = .1089 \text{ ft.}^2$$

$$C_D = .001261$$

Flat plate values of boundary layer thickness and skin friction drag coefficient.

From reference 10. $$\delta = 5.2 \sqrt{\frac{\nu}{u_o} s}$$

for $u_o = 2340$ ft. - sec.$^{-1}$

$\nu = .555 \times 10^{-3}$

$\delta = 2.530 \times 10^{-3} \sqrt{s}$

s(ft.)	δ (ft.) 10^{-3}
0	0
.025	0.397
.05	0.561
.10	0.795
.15	0.972
.20	1.124
.25	1.257
.30	1.381
.35	1.485
.40	1.590
.424	1.650

$$C_D = 1.328 \sqrt{\frac{\nu}{u_o l}}$$

$l = .415$ ft.

$C_D = .001006$

APPENDIX I

Physical Characteristics of the Model V-2 Ogive

FIG. 12 Y_o VS. X FOR V-2 MODEL OGIVE

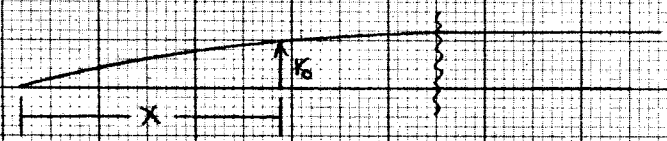

Y_o-FT.

.07
.06
.05
.04
.03
.02
.01
0

0 .05 .10 .15 .20 .25 .30 .35 .40

X – FT.

Development of an Analytic Expression for r_o (s)

(Equation 32)

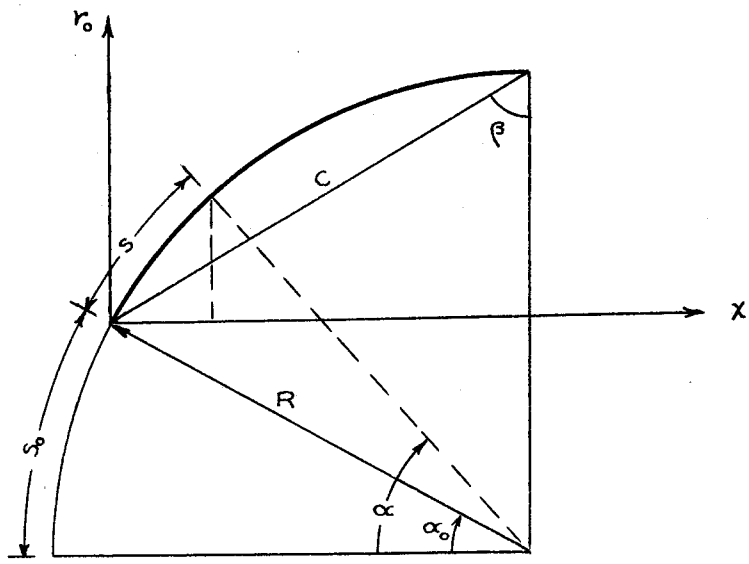

From data $r_{o\,max} = 0.061$ ft. @ $x = 0.415$ ft.

$$C = \sqrt{(0.061)^2 + (0.415)^2} = 0.419$$

$$= \tan^{-1} \frac{0.415}{0.061} = 81.65^\circ$$

R = Radius of curvature

$$R = \frac{C}{2} \frac{1}{\cos \beta} = 0.2095 \times \frac{1}{0.1454} = 1.44 \text{ ft.}$$

$$\alpha_o = \sin^{-1} \frac{R - r_{o\,max}}{R} = \sin^{-1} \frac{1.44 - 0.061}{1.44} = 73.13^\circ$$

$$s_o = R\alpha_o = 1.44 \times \frac{73.13}{57.28} = 1.840 \text{ ft.}$$

(1) $$s + s_o = R \frac{\alpha^\circ}{57.3}$$

(2) $$r_o = R \sin\alpha^\circ - (R - r_{o_{max}}) = R(-1 + \sin\alpha^\circ) + .061$$

From (1) $\alpha^\circ = \frac{57.3}{R}(s + s_o)$. Substituting this expression for into (2) we obtain the following for $r_o = r_o(s)$:

$$r_o = R\left[-1 + \sin\frac{57.3}{R}(s + s_o)\right] + 0.061$$

$$= 1.44 \sin\frac{57.28}{1.44}(s + 1.840) - 1.44 + 0.061$$

$$r_o = 1.44 \sin(39.8\, s + 73.13)^\circ - 1.379 \qquad (32)$$

$$\frac{dr_o}{ds} = \frac{1.440}{57.30} \times 39.8 \cos(39.8\, s + 73.5)^\circ$$

$$\frac{dr_o}{ds} = \cos(39.8\, s + 73.13)^\circ$$

Wetted Area of Ogive

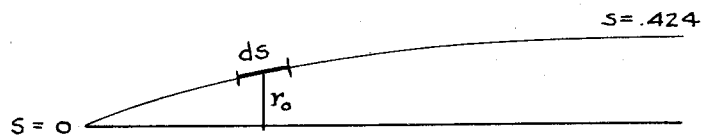

$$A = \int_o^{.424} 2\pi r_o \, ds$$

$$r_o = 1.44 \sin(39.8\, s + 73.13)^\circ - 1.379 \qquad (32)$$

$$A = 2.88\pi \int_o^{.424} (\sin(39.8\, s + 73.13)^\circ - 1.379)\, ds$$

$$A = 0.1089 \text{ ft.}^2$$

Angle of Tangent, β , to the Ogive

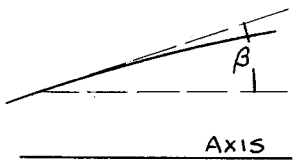

$$R(\alpha - \alpha_o) = s \qquad \beta = \frac{\pi}{2} - \alpha$$

$$R\left[\left(\frac{\pi}{2} - \beta\right) - \alpha_o\right] = s, \quad \alpha_o = 73.13^\circ$$

$$R = 1.44 \text{ ft.}$$

Then $\beta = (16.9 - 39.8\ s)^\circ$

TABLE XVIII $r_o \cos\beta$

S	$\cos\beta$	r_o	$r_o \cos\beta$
0	—	0	0
.025	.9617	.0065	.00624
.050	.9664	.0130	.01163
.100	.9748	.0244	.0238
.150	.9819	.0351	.0345
.200	.9879	.0434	.0429
.250	.9926	.0505	.0501
.300	.9962	.0560	.0558
.350	.9987	.0590	.0589
.400	1.000	.0607	.0607
.424	1.000	.0610	.0610

TABLE XIX $\dfrac{\int r_o^2\,ds}{r_o^2}$

S	r_o	r_o^2	$\int_0^S r_o^2\,ds$	$\dfrac{\int r_o^2\,ds}{r_o^2}$
		10^{-4}		
0	0	0	0	0
.025	.0065	.421	.00362	.01006
.050	.0130	1.69	.03022	.01790
.100	.0244	5.95	.2206	.0371
.150	.0351	12.30	.6765	.0550
.200	.0434	18.80	1.4544	.0775
.250	.0505	25.50	2.584	.1013
.300	.0560	31.40	4.009	.1275
.350	.0590	34.60	5.659	.1634
.400	.0607	36.90	7.470	.2025
.424	.0610	37.10	8.358	.2250